Quantification of the swelling as a result of knee pathology by wearable set-up

Hamada, Wael

Award date:
2021

Quantification of the swelling as a result of knee pathology by wearable set-up

Author:
Wael Hamada

Supervised by:
Prof. Rik Vullings (TU/e)
Dr. Alessandra Galli (TU/e)
Eng. Heleen Boers (IMEC-NL)

A thesis presented for the degree of
master in Embedded systems

Computer science and electrical engineering
Technical University of Eindhoven
The Netherlands
29th of June 2021

Summary

Monitoring and assessing the recovery of the knee after a surgery or an injury is usually done by trained physiotherapists. This assessment is mainly subjective, does not always reflect the actual recovery state of the knee, and can not detect inflammation at its early stages. In this work, the basis of a wearable device to measure and analyze the impedance of the knee to quantify the inflammatory response is proposed. We tested and evaluated the feasibility of using two of IMEC's embedded wearable platforms. The Oxpecker platform is integrated with the MAX30001 from Maxim Integrated with a frequency range between $125Hz$ and $128kHz$. And the Nightingale v2 with a frequency range of $2kHz$ to $1MHz$.

The comparison between the equivalent circuit model and the mathematical model was performed to evaluate the measurement error, which highlights that the Nightingale V2 platform performed much better than the Oxpecker. In the latter, only frequencies $> 8kHz$ had measurement error $< 10\%$ and is, therefore, found acceptable to be used. Moreover, the potentials of using the Impedance Ratio (IR) as a metric for knee joint health without the need of having a baseline measurement are discussed.

In this thesis, different types of electrodes are investigated by measuring multiple times the difference between the bio-impedance measured on both knees on a healthy subject. The results suggest the feasibility of employing conductive textiles as electrodes for this application. In addition, the Oxpecker is employed to measure the differences between two subjects: one subject with no known knee pathology history and another subject with a 10-month-old torn meniscus. The obtained difference in impedance is noticeable, even if is small due to the narrow frequency range of the Oxpecker. It was expected to have more accurate results if tested with hardware capable of injecting current at frequencies higher than $128kHz$, such as the Nightingale v2.

To measure the precision of the setup and the feasibility of using bio-impedance not only to detect the presence of swelling in and around the knee area but also to quantify the volume of the additional fluid accumulated in the knee as a result of the inflammatory response, two Ex-Vivo experiments were set up and performed on porcine models. From the results, it was proven that it is possible to detect as low as $2ml$ change in fluids using bio-impedance. In addition, we discuss the difference in reactance at frequencies higher than $200kHz$ between a bony and a boneless porcine model.

The data acquired from the latter experiments were then pre-processed and used

in regression and statistical analysis. Two main uses-cases are explored: in the first, the healthy contralateral knee was used as a baseline for the evaluation of the inflammation of the injured knee. On the other hand, the second scenario refers only to the injured knee, and its bio-impedance characteristics. In addition, the added accuracy of using instruments with a wide versus narrow frequency range for this application is explored. Moreover, Linear, Neural networks, and Tree models in multiple configurations are tested. As results, it is shown that it is feasible to fit mathematical models to predict the volume of the swelling for the use-case which considers the healthy knee as a reference with an overall $R^2 = 0.92 \pm 0.0455$ while the results for the use case without the healthy knee indicates that further analysis and different methods should be explored to remove the for a baseline measurement as the overall $R^2 = 0.51 \pm 0.348$.

In addition, to achieve the end goal of a truly wearable and easy to work with setup, and to standardize the measurements further, a custom knee brace with integrated electrodes made of conductive fabric is proposed, designed, and implemented. Moreover, the custom brace is tested on a group of 10 patients with known knee pathology in collaboration with St. Anna hospital in Geldrop/ Eindhoven, the Netherlands. In the majority of cases, a clear lower impedance is observed when comparing the injured knee to the healthy contralateral knee. To evaluate the repeatability of the measurements acquired using the knee brace, each test was repeated three times, the overall standard deviation was 0.268Ω. Additionally, the fitted coefficients from the regressional analysis are used to try to predict the volume of swelling in ml, the results obtained are correlated to the expert assessment of the patients, for example, the highest volume of predicted swelling of $17.3ml$ was for the patient which the swelling was scored the worst by the expert.

Finally, to conclude, in this work, we have proven that it is feasible to develop a wearable that can be used to evaluate the status of a knee joint after an inflammatory response using bio-impedance. We also show that it is feasible to build a mathematical model to predict the volume of fluid accumulated in the knee, which is expected to provide a more objective assessment compared to the current assessments that are highly dependent on physiotherapists. Moreover, for a truly wearable system, we show that is it possible to use conductive fabric attached to a knee brace to eliminate the burden of using the traditional pre-gelled single-use electrodes.

Acknowledgements

Over the last seven months, I was fortunate to work on this master thesis in an outstanding atmosphere in IMEC-NL with the support of the Signal Processing Systems (SPS) group at the Technical University of Eindhoven and backed up with medical support from St.Anna hospital in Geldrop. The opportunity has been an incredibly delightful and fun experience where I've learned a lot over combining embedded engineering and problem-solving skills in the healthy and medical domain.

I would like to thank all people who contributed to this work, especially my IMEC coach and supervisor Heleen Boers for guiding me through the project, making sure I have everything I need to successfully accomplish each step, and giving me a lot of her knowledge and experience on setting up and executing experiments.

I would like also to thank Alessandra Galli and Rik Vullings from the TU/e for their great support, quick responses, and fruitful discussions. They made sure I stay on track and focused on my assignment and its scientific aspect and helped me with any practical questions as well.

I am thankful to St. Anna Hospital and especially Walter van der Weegen from the department of Orthopaedics for the guidance, answering questions, and providing necessary information regarding the medical side of the project.

Many people at IMEC-NL Health have also contributed to this thesis. This work would not be possible without their critical feedback, willingness, and being open to answering any of my questions. I truly appreciate every moment they took to help overcome all obstacles.

Finally, the biggest thanks go to my family who has always been beside me.

Contents

Chapter 1

Introduction

Knees, hips, and ankles are the joints that bear the most weight in our body, unlike hips and ankles, knees do not have the stability procured by the joint congruity and they are therefore more frequently injured than any other joint in the human body [Casteleyn, 1999], However, not only the biological evolution of humans as species are to blame for knee injures, a study analysed 25 years of sports found a strong correlation between knee injuries and the public interest into relatively recent sports such as skiing, skating and mountain-biking [Steinbrueck, 1999]. While [Hootman et al., 2002] suggested developing and implementing programs to moderate active adults in order to prevent knee injuries, monitoring injured knees during the period after a medical intervention can also improve the recovery of the joint [McDonald et al., 2012].

1.1 Problem description

A local inflammatory response in the knee area is normal and expected in patients with knee pathologies and after surgeries such as a Total Knee Arthroplasty (TKA) or an Anterior Cruciate Ligament (ACL) reconstruction. It is in most cases combined with some mild pain and dysfunction, but it can also escalate to moderate or severe pain in up to 30% of the patients for a duration of multiple weeks [Aasvang et al., 2015] which might indicate more serious problems [Lieberman et al., 2021].

Currently, the assessment of the knee recovery is done by trained physiotherapists in intervals by visually inspecting and feeling the knee to identify the presence of the main symptoms of inflammation such as by feeling an increase in local temperature [Denoble et al., 2010], comparing the circumference of the knee [Jakobsen et al., 2010], and by dynamically sensing the movement of the fluid across the knee with special techniques like the Bulge sign, Patellar tap, and sweep tests [Wang et al., 2019] [Maricar et al., 2016]. However, those methods can be very subjective and are not suitable to detect the early stages of inflammation. Especially the fluid in the knee (swelling) is hard to assess, as the volume of the swelling can be too small, located inside the knee capsule, and therefore hard to be detected by physiotherapists.

1.2 Goals

The aim of this project is therefore divided into the following goals

- To study knee inflammatory response and investigate the feasibility of using off-the-shelf sensors and techniques to measure the magnitude of inflammation by focusing on the swelling and its volume during the recovery period.
- To study the feasibility of developing a wearable for monitoring of knee swelling that can be used the patient him/her self at shorter intervals.
- To quantify the precision expected from the wearable.

1.3 Outline

In this paper, a base of a non-invasive wearable battery-powered low-cost device to measure the inflammation of the knee is presented. Along with a proposal of a custom reusable knee brace with integrated electrodes. In this work, we focus on testing the feasibility and the precision of multi-frequency bio-impedance in detecting and quantifying the swelling by measuring the volume of additional fluid in and around the knee area which will allow a more objective way to quantify the recovery of a knee joint and can be used by the patient himself at home at shorter intervals to get more detailed insights during the recovery period.

Furthermore, we conducted ex vivo tests on porcine models to mimic different intensities of swelling in order to fit a regression model that can be used to predict the specific amount of fluids in a swollen knee. Along with investigating the impedance ratio at higher over low frequencies as a technique that improves the convenience of the setup by removing the need to use the healthy knee as a baseline to the injured knee.

Chapter 2 focuses on the medical point of view on the knee anatomy and the main symptoms of the inflammatory response after an injury or surgery. Furthermore, the chapter introduces the background of the impedance analysis techniques. In particular, it focuses on the path the electrical current will travel through in a biological medium and the effect changing the frequency of injected current has on the path of the electrical signal through the medium, the common and the most recent techniques used to measure the health of a biological medium using bio-impedance.

Chapter 3 provides an overview of the used hardware and the proposed techniques with thorough verification of the behavior of the system compared to a Simulink simulation and to a mathematical model. It also presents the method used to select the frequency range of the experimental setup. In addition, this chapter also discusses choosing the right type of electrodes and investigates the use of the simple ESD bands as flexible reusable electrodes.

Chapter 4 describes two ex vivo experiment performed on porcine models where an amount of fluid is injected into the models at small steps and bio-impedance was measured at each step to build a dataset that is then used in regressional and

statistical analysis to evaluate the feasibility of using fitted mathematical models to predict the volume of added fluid from bio-impedance characteristics.

Chapter 5 proposes a custom knee brace design with integrated electrodes made of conductive fabric. Furthermore, in collaboration with St.Anna hospital in Geldrop/ Eindhoven, the custom knee brace is evaluated on ten patients with known knee pathology and the results are compared to the assessment of an expert physiotherapist.

Finally, Chapter 6 concludes this work and provides suggestions to a future related work.

Chapter 2

Background and related work

The main symptoms of an inflammatory response in the knee are pain, stiffness, an increase in the local temperature, and swelling. The latter occurs when fluid accumulates in or around the knee joint. It mainly starts in the capsule as well as around the patella and can in advanced stages spread to the surrounding tissues [Roemer et al., 2016].

Up until now, the evaluation of the recovery of the knee is usually done by expert

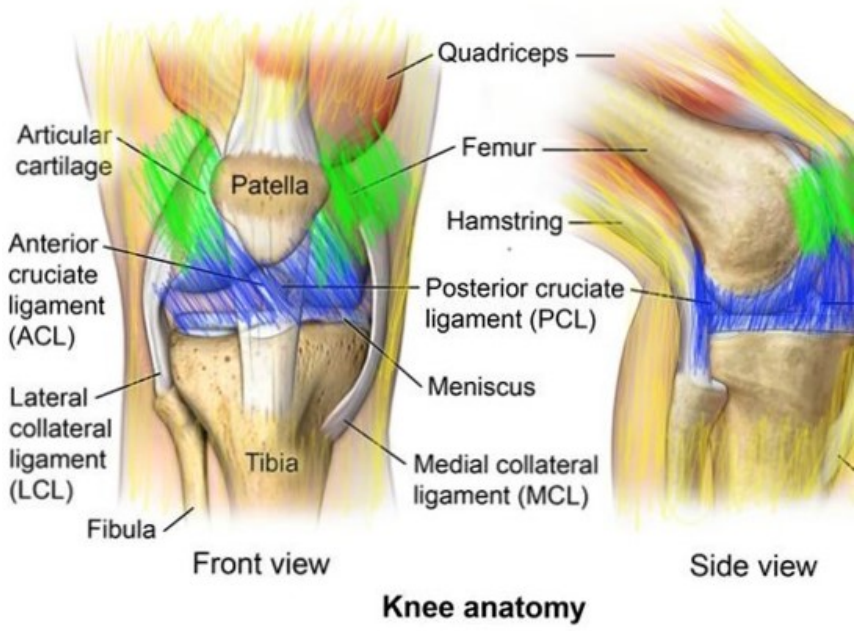

Figure 2.1: Knee anatomy with 3 main highlighted areas, a) In blue, in-capsule area. b) In green, the area surrounding the Patella. c) In yellow, the surrounding tissues. **Source:** https://comportho.com/anatomy/anatomy-of-the-knee/

physiotherapists, they use techniques such as *The Bulge Sign*, *Patellar tap*, and *Sweep tests* [Wang et al., 2019] [Maricar et al., 2016] to examine the knee by feeling the movement of the fluids around the knee area. Those methods only provide some indication of the presence of fluids and they can not be used to quantify the volume of the swelling. Moreover, depending on the level of experience a physiotherapist has and the location of the swelling, the results can be very subjective, such as if the swelling is inside the knee capsule and at small volumes, physiotherapists might

not be able to detect it.

There are more accurate methods to quantify the volume of swelling, but they usually either invasive as in Arthroscopic Evaluation [Zschäbitz et al., 1992] or uses MRI and image processing, such as the Knee Inflammation MRI Scoring System (KIMRISS) [Jaremko et al., 2017]. In this work, we will investigate the use of impedance analysis to non-invasively quantify the volume of the swelling in the knee area.

2.1 Impedance analysis and magnitude $\mid Z \mid$

One of the non-invasive techniques to analyze the composition and structure of an object is impedance analysis [Instruments, 2007] which is based on the injection of an alternating electrical current into the object and measuring the voltage drop, where a higher drop indicates higher material resistivity. Bio-impedance is a similar technique but with a very low current injected into the biological medium.

Impedance (Z) can be defined as the opposition of an electrical system to the flow of electric current and it has two components [Weik, 2001]: Resistance (R) and Reactance (X_c). R can be defined by the amount of current the medium will block [Weik, 2001]. For example, fat is known to be an excellent resistor to electrical current, so tissues with high fat composition will have higher resistivity than tissues with high water content like blood, muscle, and fluids around the cells. The X_c can be defined as the medium's ability to slow down the current [Weik, 2001]. That is best noticeable for instance around the membrane of the cells as it can store the charges for a short time and therefore slowing the current [Roa et al., 2013].

2.2 ECW and ICW

Biological mediums are generally composed of extracellular water (ECW) and cells. Each cell has intracellular water (ICW) and a membrane around it, and the Total Body Water (TBW) content is, therefore, the sum of ICW and ECW. The membrane of the cells acts as a thin insulator between two more electrically conductive materials hence, the ICW and the ECW [Golowasch and Nadim, 2013]. This characteristic practically makes the cell's membrane act as an electrical capacitor for the electrical current injected into the biological medium. Knowing that it is possible to model this composition electrically as a circuit with a capacitor and resistor in series connected to a resistor in parallel, see Figure 2.2, in which, R_i and R_e represent the resistivity of the Intracellular and the Extracellular body water respectively while C_m represents the capacitance of the cell membrane.

2.3 Frequency range

Many standard off-the-shelf bio-impedance devices inject the current at a fixed frequency usually at 50kHz to measure the impedance of the biological object as in [Loyd et al., 2020]. However, more information can be gathered about biological tissues by analyzing the dispersion effects from the interaction of electromagnetic radiation with the ECW and body cells. In which, a current injected at low frequency

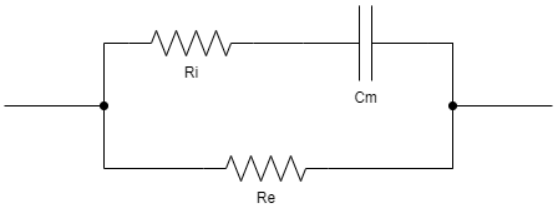

Figure 2.2: An electrical equivalent circuit representing a simple biological cell where R_i, R_e, and C_m symbolizing the resistance of the intracellular water (ICW), the resistance of the extracellular water (ECW), and the capacitance of the cell membrane, respectively.

is more likely to travel through the ECW and around the cells as the membrane does not allow current to permeate the cells, while if injected at high frequency, the capacitive effect of the membrane increases which allows the current to travel through the cell's membrane and ICW, see Figure 2.3.

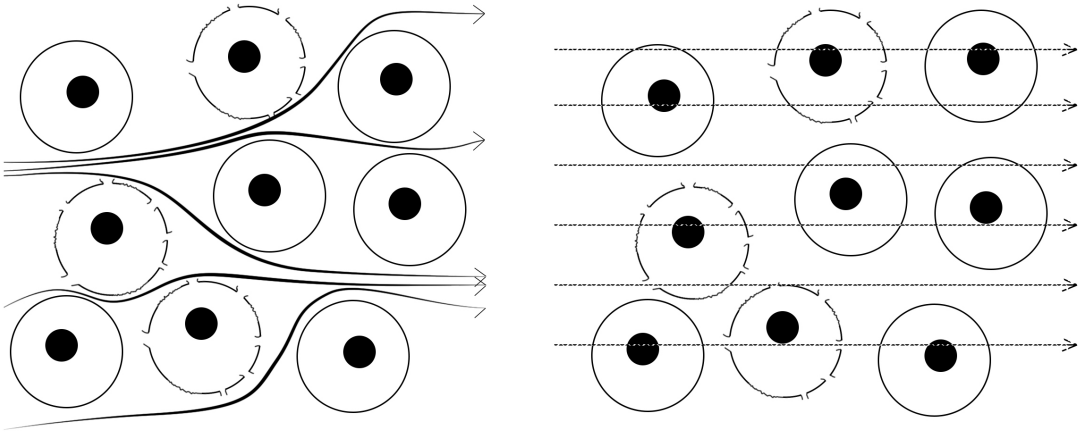

(a) (b)

Figure 2.3: Electrical current traveling trough the Extracellular Water ECW in (a) at low frequencies and through the ECW, the cell membrane and the Intracellular water ICW in (b) at high frequencies

In the literature, three main frequency ranges are defined [Gabriel et al., 1996]: α, β, and γ with ranges of [10 Hz - 10 kHz], [10 kHz - 100 MHz] and [100 MHz - gigahertz's], respectively. Only few attempts of analysing the α range on human were successful [Grimnes and Martinsen, 2010] compared to the β range. Mainly because the α range is more sensitive to the type of electrodes and wires used [Mellert et al., 2011].

One of the most common ways to visualize the complex impedance Z and its real part R and complex part X_c is using a Nyquist plot of the 2-d complex plane illustrated in Figure 2.4. The intersection of impedance Z as a function of frequency f with the x-axis ($Real(Z)$) represents the resistance of the ECW (R_e) when the current is injected at very low frequency $R_0 = R(f \to 0) = R_e$ and the resistance of the composition of the ECW and the ICW (also known as the TBW Resistance) when the current is injected at very high frequency $R_\infty = R(f \to \infty) = \frac{R_i R_e}{R_i + R_e}$

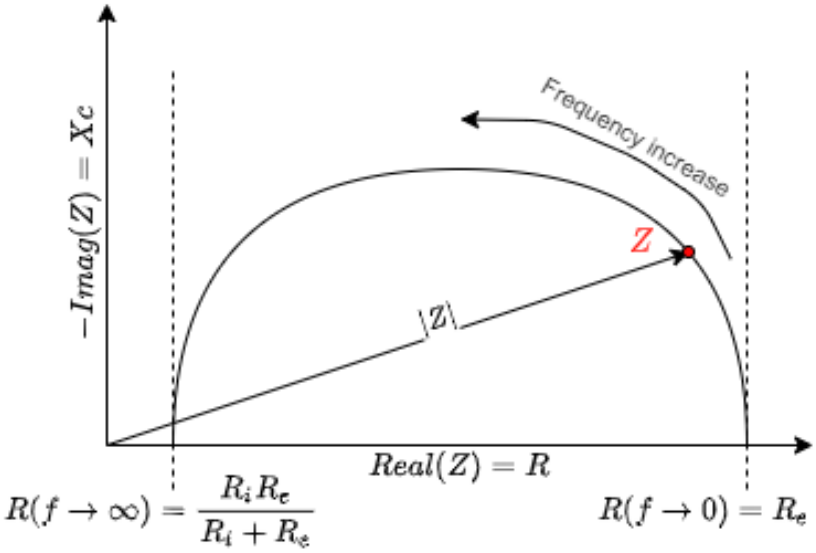

Figure 2.4: Nyquist plot showing the impedance Z and its magnitude $|Z|$ as a function of frequency f in the complex 2-d plane.

2.4 Impedance Ratio (IR)

Most current bio-impedance analysis techniques are based on linear regression [Muller et al., 2020] using parameters highly dependent on the studied population group and include other components such as age, gender, ethnicity, and weight. To eliminate those factors, the impedance ratio (IR), a relatively recent method, was introduced by the European Society for Clinical Nutrition and Metabolism (ESPEN) [Rinninella et al., 2018]. IR is a metric to quantify the health condition of the cell membrane, by taking the ratio between Z at high frequency to Z at low frequency. The higher the ratio the more "solid" the membrane. While if the variance is low, then it is an indication of an unhealthy cell membrane allowing the leakages of fluids between the ICW and the ECW. The ideal upper and lower frequencies for the IR are in theory the frequencies of R_∞ and R_0 respectively, see Figure 2.4. In Chapter 4 the selection of frequencies for IR will be discussed further.

Chapter 3

Materials and methods

Since one of the main requirements of the target setup is to remain wearable and portable, a small platform/device that can inject current and measure the impedance at certain frequencies is needed. Oxpecker and Nightingale [Lee et al., 2019] are examples of Imec's custom hardware platform that can be modified to suit a wide range of medical applications.

In this chapter, we will discuss the available platforms, explaining the reason for preferring one over the other, describing the approach taken to test the performance and accuracy and make a decision on the platform to be used for this setup.

3.1 IMEC's Oxpecker platform

The Oxpecker is one of the more modular platforms being developed for research work within IMEC. At just around 7x7x2cm with the battery, it is small, portable enough to be used in wearable applications see figure 3.1. It is equipped with a MAX30001 IC from Maxim Integrated, Bluetooth low energy (BLE), and uses universal interfaces such as COM and HDMI standard connectors which makes prototyping much easier.

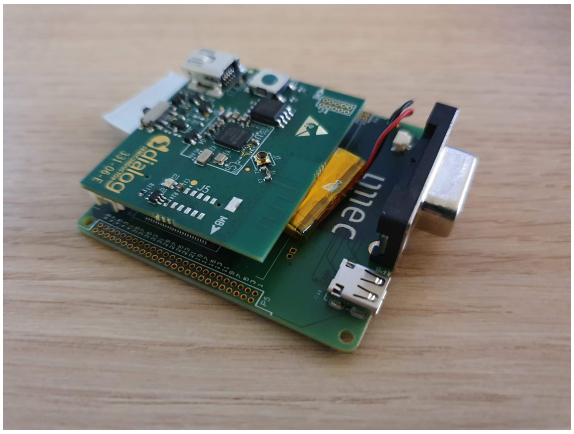

Figure 3.1: A photograph of IMEC's Oxpecker platform

To connect the bio-impedance electrodes, the Hippo, a connector board with five electrode leads is used. It is equipped with a standard HDMI interface as shown in (figure 3.2).

The MAX30001 IC integrated into the Oxpecker has a single bio-impedance channel and is capable of injecting a current from $8\mu A$ to $96\mu A$ at 11 different frequencies ranging from 125 Hz to 128 kHz using both 2 or 4 electrode setups.

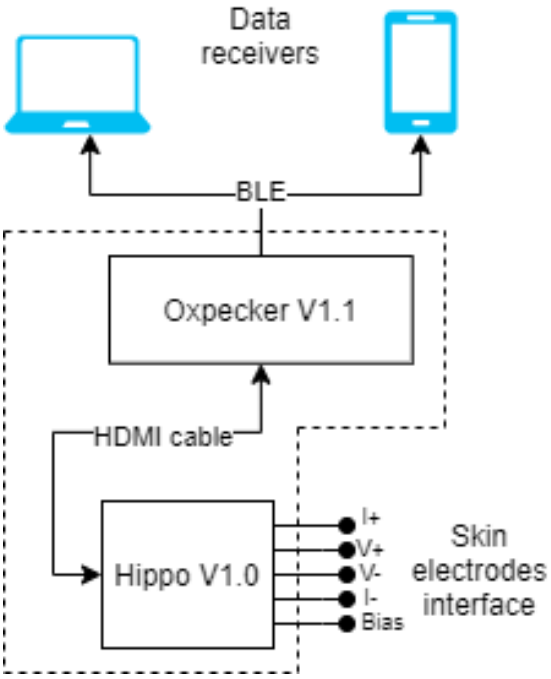

Figure 3.2: System block diagram.

3.2 Testing and verifying the setup (Oxpecker)

Because the system consists of multiple parts being integrated and embedded together, is important to verify the behavior and the results from this setup to ensure that the setup is functioning as expected. To do this, the same bio cell RRC equivalent circuit from figure 3.3 is used in physical, mathematical, and simulation setups to analyze the accuracy of the measured impedance and calculate the error. The setups were tested with a fixed R_i of $100 \pm 5\%\Omega$, a C_m of $4.7e-8 \pm 10\%F$ and a variable R_e of $[0, 47, 100, 220, 560, 1200] \pm 5\%\Omega$ to represent different composition of fluids in the ECW varying in type and/or amount.

3.2.1 Simulation

In Impedance analysis, both the voltage and the current are time-dependent sinusoidal functions. Therefore, by measuring the voltage and the current, the impedance can be calculated as $Z(t) = V(t)/I(t)$. knowing that the phasors of the voltage $V(t) = V_0 cos(\omega t)$ and current $I(t) = I_0 cos(\omega t + \varphi)$ where ω is the radial frequency given by $\omega = 2\pi f$ where f is the frequency of the injected current in Hz, in-which, if the system has no phase shift ($\varphi = 0$), the impedance Z will be reduced to the well-known Ohm's law $R = V/I$. To simulate this in Matlab Simulink [MATLAB, 2021], a current generator is used to inject a current at a

specific frequency to an equivalent circuit while the voltage and current are measured and used to calculate the impedance (figure 3.3).

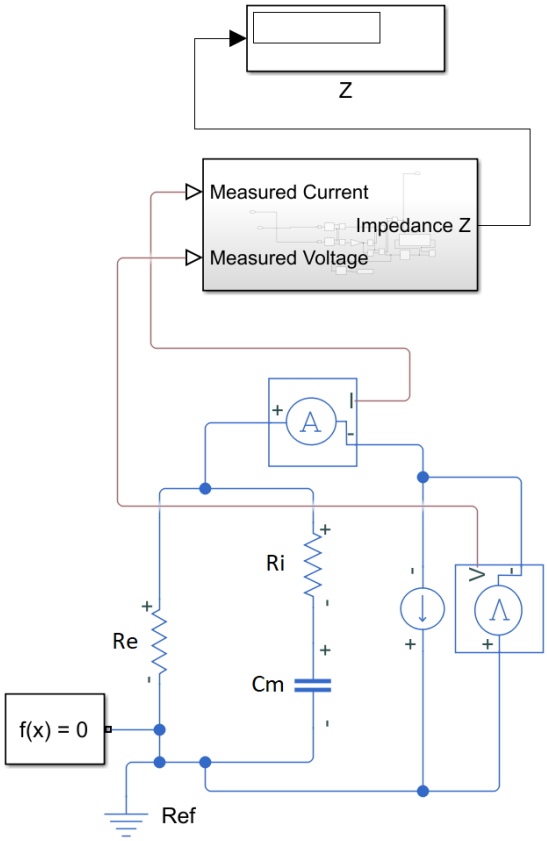

Figure 3.3: a Simulink model consists of an electrical model representing an equivalent circuit of biological tissue, a current generator, current/voltage sensors, and a subsystem to calculate the impedance of the simulated model

3.2.2 Mathematical model

Knowing that the impedance of an ideal resistor R is given by $Z(R) = R$ and the impedance of an ideal capacitor C is given by $Z(C) = 1/j2\pi fC$ [Harres, 2013], the total impedance Z of the equivalent circuit, i.e., R_e in parallel to C_m and R_i in series, can be mathematically calculated according:

$$Z = \frac{R_e(R_i + \frac{1}{j2\pi fC})}{R_e + R_i + \frac{1}{j2\pi fC}} \tag{3.1}$$

where f is the frequency of the injected current in Hz and j represents the 90° phase shift of the capacitor.

Rearranging the terms and separating the real and imaginary parts of the complex impedance Z [Azar, 2012] reduces the $Real(Z)$ and the $Imag(Z)$ respectively to:

$$Real(Z) = R = R_\infty + \frac{R_0 - R_\infty}{1 + (2\pi fC)^2\tau^2} \tag{3.2}$$

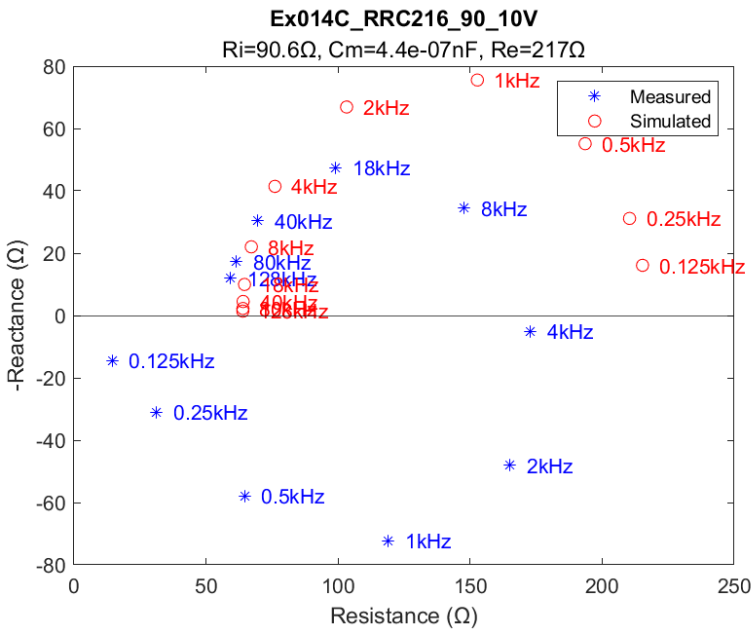

Figure 3.4: A Colecole representation showing the Resistance and Reactance measured using the Oxpecker compared to the simulated values when tested with an RRC equivalent circuit of $R_i = 90.6\Omega$,$C_m = 47nF$, $R_e = 217\Omega$

$$Imag(Z) = Xc = -\frac{2\pi f C\tau(R_0 - R_\infty)}{1 + (2\pi f C)^2\tau^2} \tag{3.3}$$

where τ represents the time constant of the circuit and given by $\tau = (R_e + R_i)C$.

3.2.3 Setup verification results and frequency range selection

By using the nominal values of the components in the physical RRC circuit - see Figure 3.5 - were used in the mathematical model, Table 3.1 shows the error percentage of the measured to calculated resistance, and Figure 3.4 shows the difference between the measured and simulated values on a Colecole representation. It is noticeable that the system accuracy is higher at high frequencies where it drops significantly at frequencies of lower than 8 kHz with average measurement errors larger than 10%. Many attempts are made to debug this behavior/error, by, for example, bypassing the Hippo connector board and the HDMI interface (Figure 3.5) but that made only a very marginal difference to accuracy. Further analysis is needed to debug this behavior as the problem could be inherited in the MAX30001 itself.

Only frequencies 8 kHz and higher on the Oxpecker platform will be employed for this project, since these frequencies are accurate enough to have an acceptable measurement and that most of the bio-impedance applications use frequencies in the β dispersion frequency range of [10 kHz - 100 MHz] [Roa et al., 2013].

Table 3.1: The error percentage of measured to calculated resistance R of an RRC equivalent circuit illustrated in Figure 3.3, injected with a current at multiple frequencies tested with fixed Cm and Ri of $47nF$ and 90Ω respectively and multiple Re resistances.

Frequency	*Current* (μA)	Measured vs calculated R error (%)					
		$Re = 47\Omega$	$Re = 100\Omega$	$Re = 220\Omega$	$Re = 550\Omega$	$Re = 1200\Omega$	*Avg Error (%)*
128 kHz	48	8.53	7.70	7.81	8.15	8.34	8.10
80 kHz	48	7.88	6.82	6.78	7.02	7.09	7.12
40 kHz	48	7.90	6.48	5.81	5.33	5.06	6.11
18 kHz	48	9.34	7.81	5.56	1.90	0.45	5.01
8 kHz	48	10.80	10.35	9.48	2.78	6.66	8.01
4 kHz	32	12.87	12.35	12.61	8.42	4.65	10.18
2 kHz	16	22.29	21.31	21.28	19.84	10.89	19.12
1 kHz	8	44.78	43.70	49.00	42.95	39.62	44.01
500 Hz	8	69.76	69.11	68.93	68.86	68.22	68.98
250 Hz	8	84.88	84.51	84.42	84.43	84.35	84.52
125 Hz	8	92.34	92.25	92.18	92.22	92.21	92.24

3.3 IMEC's Nightingale V2

The NGv2 (Nightingale V2) [Lee et al., 2019] is one of the new ultra-low-power multi-sensor platforms designed by IMEC with the goal of being used for researches in the wide wearable health and medical domain. The NGv2's SoC includes ECG, Bio-impedance, PPG, and interfaces to add more sensors, integrated with a 500mAh 3.7V battery in a compact form factor see Figure 3.6. The bio-impedance component of the NGv2 supports frequencies between $1kHz$ and $1MHz$, it can be configured to do multi-frequency bio-impedance measurements by selecting a number of frequencies to continuously cycle between the selected ones to complete measurement sweeps.

3.3.1 NGv2's Performance

Evaluated using the same evaluation method as used with the Oxpecker in the previous section, The bio-impedance measurements acquired using the NGv2 on the other hand were much more accurate when compared to the simulated expected results as shown in Figure 3.7. The complete results and comparison between the

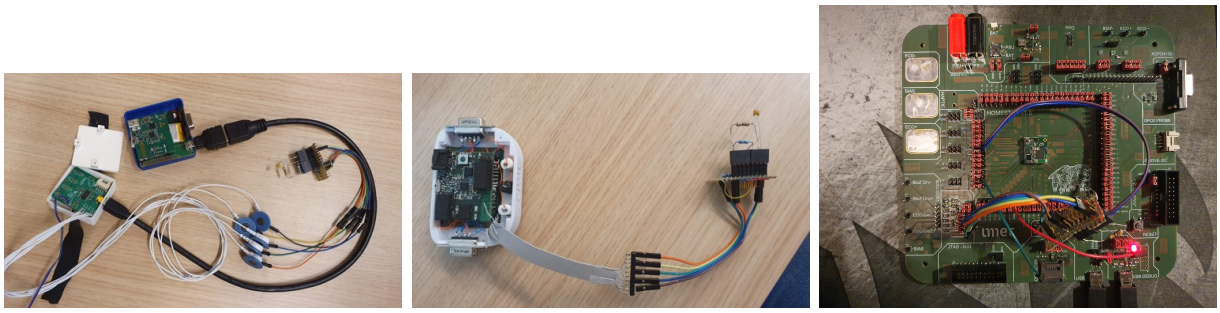

(a) (b) (c)

Figure 3.5: Testing the device with an RRC equivalent circuit. (a) is a complete setup, showing the Oxpecker connected to the Hippo connector board using an HDMI interface and the test board with the equivalent circuit connected using clips to the electrodes. (b) is a minimal setup bypassing some components and wiring. (c) the Homester, an Oxpecker devboard used in debugging the issue

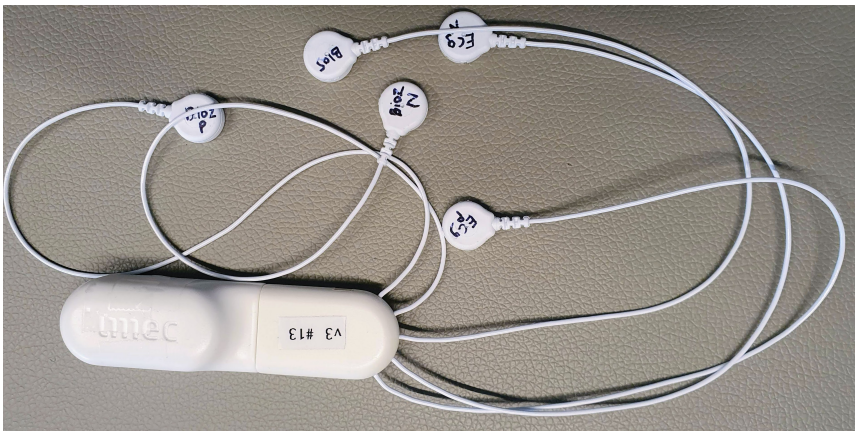

Figure 3.6: A photograph of IMEC's Nightingale V2 platform.

NGv2 and the Oxpecker in terms of accuracy can be found in the Appendix 7.1

3.3.2 Device choice

During the first phase of the project, IMEC's preference was to use the Oxpecker platform for this project. However, considering the results of the evaluation test provided in this section, a decision was made to switch to the NGv2 platform instead since further debugging and analysis of the issue with the Oxpecker platform will not fit within the available timeline and is out of this project's scope. In addition, the Maltron BioScan920-II bio-impedance analyzer with its multi-frequency ($5kHz$,$50kHz$,$100kHz$, and $200kHz$) is provided by IMEC to be used as a reference to the measurements.

3.4 Choosing the right electrodes

One of the most important aspects in measuring bio-impedance is the electrodes as they are the primary interface between the biological medium and the electronic system both for injecting current and for measuring the voltage changes.

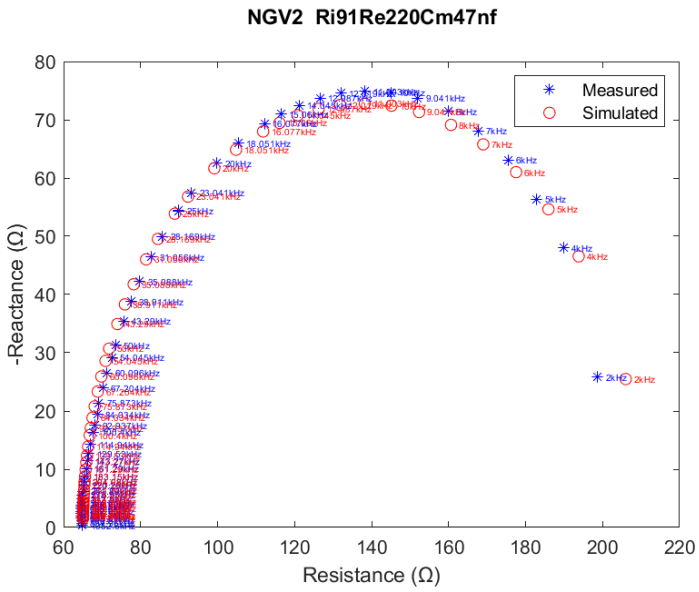

Figure 3.7: A Colecole representation showing the Resistance and Reactance measured using the NGv2 compared to the simulated values when tested with an RRC equivalent circuit of $R_i = 90.6\Omega$,$C_m = 47nF$, $R_e = 217\Omega$.

3.4.1 Types of electrodes

Disposable Pre-gelled Ag/AgCl electrodes are considered one of the best types of electrodes and are widely used in the medical industry for applications such as electrocardiogram (ECG). However, for wearable applications, the disposable pre-gelled electrodes become unsuitable as, if the wearable device is meant to be used by the patient him/herself, replacing and positioning the electrodes in the correct intended way will increase the burden on the patient and the variance in the measurement. In this section, we will investigate using the commonly known electrostatic discharge (ESD) bands as flexible off-the-shelf electrodes and compare them to dry non-gelled Ag/AgCl electrodes since they are reusable and hence more convenient for a wearable setup.

To measure the accuracy of each type of electrode, the impedance of both legs of a healthy subject is measured with the three types of electrodes. The expected difference in impedance between both legs is close to zero since the subject had no known knee problems and both legs are expected to have similar impedance and ColeCole curves. Figure 3.8 shows the estimated curve of the complex impedance on a 2-d plain and Table 3.2 shows the mean difference between the left and the right knees in (Ω). It is noticeable that for all types of electrodes tested, the higher the frequency the more accurate is the measurement comparing the results from both legs. The non-gelled Ag/AgCl electrodes see Figure 3.9b, were very hard and tricky to work with, they can perform well in very specific conditions as they only show an error of 2 Ωs when a full leg brace is used and tightened to an uncomfortable level shown in Figure 3.9. Therefore, the dry Non-gelled electrodes are deemed unsuitable for this project. On the other hand, the average error calculated from as the difference between bio-impedance measured on both knees of a healthy subject

when tested with the ESD bands around the knee shown in Figure 3.10 a, ranged between 4.19 to 2.07 Ωs at 8 and 128 kHz respectively (Table 3.2), this repeatable relatively low difference between the knees of a healthy subject concludes that the bands are potentially suitable for this project.

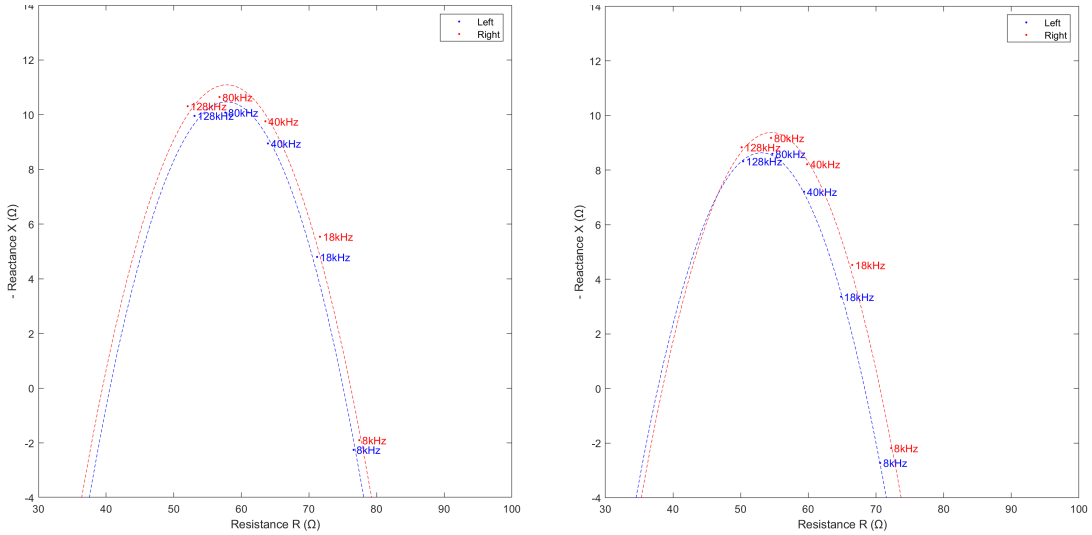

(a) (b)

Figure 3.8: Nyquist plot showing the resistance and reactance changes over different frequencies of the same subject measured with (a) Pre-gelled Ag/AgCl electrodes and (b) Band electrodes; Measured using the Oxpecker.

(a) (b)

Figure 3.9: (a) Full leg brace used in combination with the dry Non-gelled Ag/AgCl electrodes to ensure better contact with the skin. (b) A photograph of the used dry electrodes.

3.4.2 Positioning the electrodes around the knee

Positioning the electrodes is also important to target a specific part of the knee for impedance analysis. In Figures 3.10 b/c the proposed positioning of electrodes around the knee area are reported. When tested on a healthy subject with no known knee problems, very little difference in measured impedance is noticed between the diagonal and the longitudinal placements. The positioning of the electrodes might need to be tested on patients with known knee problems for further evaluation of

Table 3.2: Mean ± Standard Deviation (Min, Max) of difference in Ωs between left and right legs knees of a healthy subject with no known knee problems history using multiple types of electrodes.

Frequency	**ESD Bands**	**Non-gelled Ag/AgCl**	**Pre-gelled Ag/AgCl**
8 kHz	4.19±4.44 (1.53, 9.32)	58.12±48.66 (1.95, 87.25)	1.56±1.82 (0.01, 3.99)
18 kHz	3.41±3.10 (1.25, 6.97)	52.63±43.87 (2.00, 79.22)	1.23±1.33 (0.00, 3.00)
40 kHz	2.74±3.07 (0.83, 6.28)	46.02±38.95 (1.08, 70.01)	0.99±0.92 (0.01, 2.22)
80 kHz	2.53±3.30 (0.61, 6.34)	41.38±35.17 (0.78, 62.42)	0.94±0.80 (0.01, 2.01)
128 kHz	2.07±2.65 (0.52, 5.13)	37.04±31.11 (1.17, 56.50)	0.73±0.55 (0.00, 1.15)

the two proposed placement layouts. Furthermore, depending on the test with the ESD band, a proposal for a custom knee brace with attached electrodes made of conductive fabric will be described in chapter (5), in which, the larger surface area of and the fixed distance between electrodes on the brace will help to reduce the measurement errors caused by the inconsistent placement of electrodes.

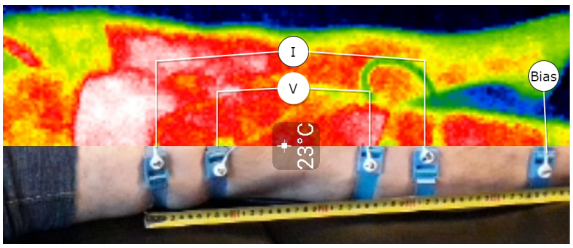

(a)

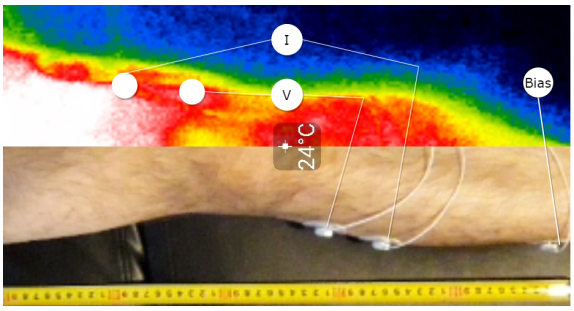

(b)

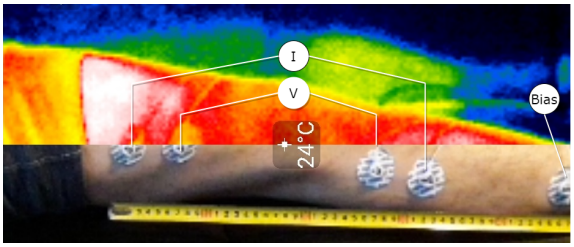

(c)

Figure 3.10: The positioning of the current injection electrodes I and voltage measurement electrodes V in (a) Bands as electrodes, (b) Gel electrodes diagonally -top view-, and (c) Gel electrodes longitudinally. The upper part shows a thermal image used to ensure a unified temperature over all experiments.

Chapter 4

ExVivo Experiments

To test the feasibility and the precision of bio-impedance when used as a metric to quantify the volume of additional fluids inside the knee joint as a result of the inflammatory response, we prepared and performed two ex vivo experiments. In both experiments, bio-impedance measurements were acquired using the NGv2 and The Maltron BioScan 920-II [Maltron International, 2021], where surface temperature was measured with a thermal camera [Seek Thermal, 2021] to ensure homogeneous temperature for the duration of the experiment. The ex vivo experiments are based on injecting a specific amount of fluid in a biological tissue and measure bio-impedance at fine steps. It is expected that the experiments will provide a dataset of measured bio-impedance and how it changes when a specific volume of known additional fluid is injected. The hypothesis is that the results can be used to fit a mathematical model to predict the volume of additional fluid (the swelling) for a measured bio-impedance.

4.1 Meat experiment 1

In the first experiment, we used a piece of boneless cooled pork with its skin still on it. While in section 3.4 we saw that ESD bands have good accuracy, Ag/Agcl pre-gelled electrodes and snap connectors were used as they are more suited for this test considering the shape and the surface of the meat piece. Electrodes were placed on the skin as shown in Figure 4.1. $40ml$ of fluids was injected in total at $5ml$ for each step. After each injection, measurements were taken using the BioScan920-II and the NGv2 separately.

Results

Figure 4.2 shows it is indeed feasible to distinguish the presence of different volumes of fluids in a biological medium by comparing the bio-impedance properties. In the first half of the experiment from 0 to $20ml$, We notice a clear and stable decrease in resistance and reactance of the tissues at all frequencies. However, as snap electrodes and button connectors were used, alternating between the devices for each measurement led to the need to replace the electrodes halfway during the experiment. At that point, the medium surface was noticeably wet which resulted in less accurate results for the measurements between 20 and 40ml.

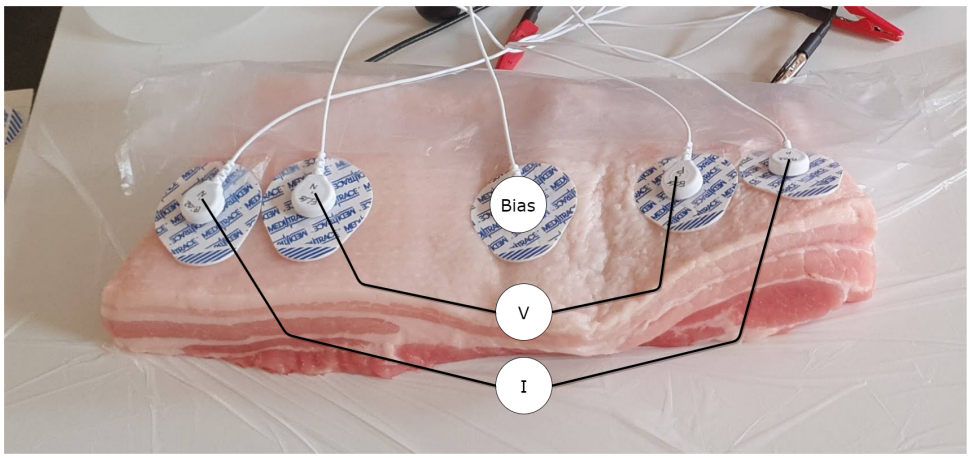

Figure 4.1: The placement of the electrodes on biological medium for the first meat experiment.

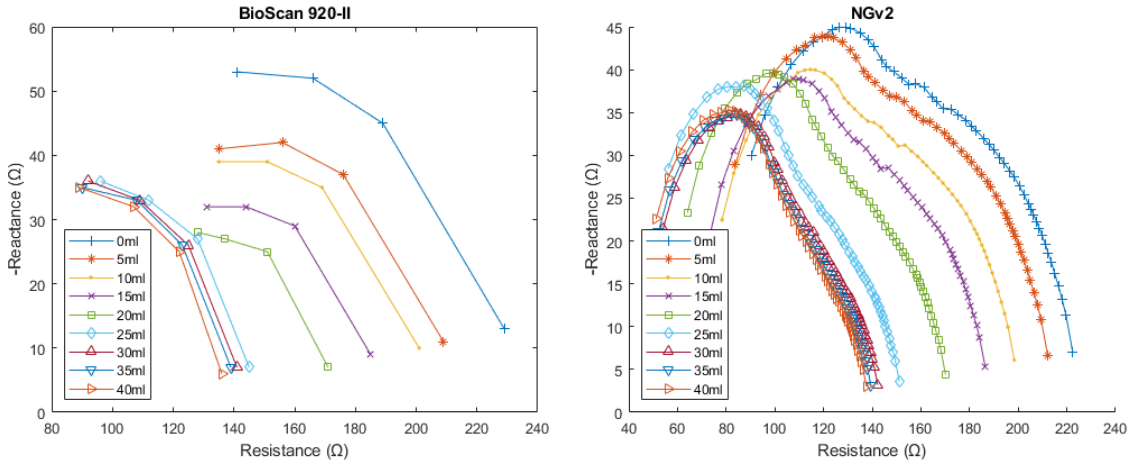

(a) (b)

Figure 4.2: ColeCole plots showing the measured Resistance R and Reactance X of the Meat experiment 1 for each injection step. acquired using: (a) using the The Maltron BioScan 920-II, (b) The NGv2

4.2 Meat experiment 2

After the success in the first meat experiment, and to gather a more accurate and larger dataset, we re-performed the last experiment in a more controlled way and using a medium that can represent a human knee more accurately. For that, a freshly cut pig's whole foreleg is used as it contains skin, muscle, and bones. Electrodes were placed on the skin as shown in Figure 4.3 and wrapped with tape to ensure consistent and better electrode-to-skin contact throughout the whole experiment. In addition, small cuts in the tape were made to allows us to access the electrodes' snap connectors. Small crocodile extension wires were made and used to avoid putting too much strain on the electrodes' heads when switching between devices. Furthermore, $80ml$ of 0.9 NaCl at steps of $2ml$ were injected, and for each step, the temperature is measured using a thermal camera.

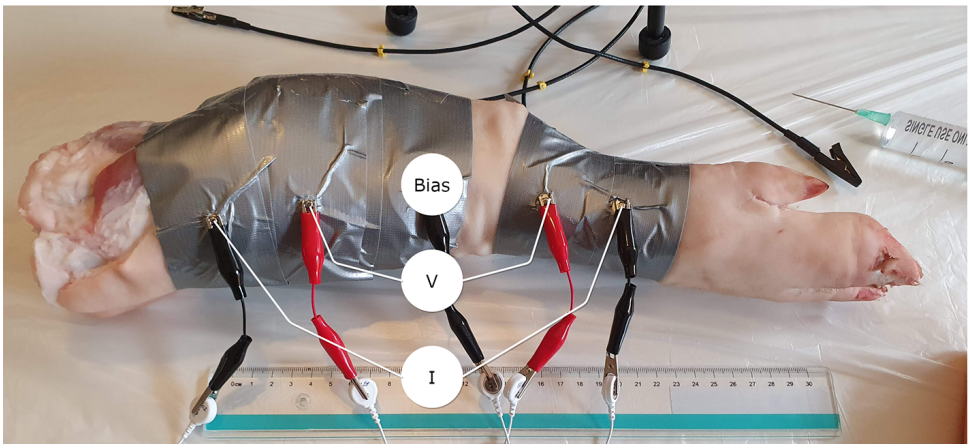

Figure 4.3: The placement of the electrodes on biological medium for the second meat experiment.

Results and Discussion

Similar to the results from the first experiment, the reduction in measured resistance and reactance after each injection step is steady and distinguishable for both measurements acquired using the BioScan920-II and the NGv2 as shown in Figure 4.4. Furthermore, It is visible that the reactance measured in both experiments has different characteristics when current injected at frequencies higher than $200kHz$. When compared closely in Figure 4.5, the reactance measured in the second experiment had a second bump compared to the first experiment. In chapter 2 we discussed how capacitance is related to the membrane of biological cells. Moreover, confirmed by a bio-impedance expert, because the second bump in reactance is at high frequencies, it is expected to be related to the bone inside the used medium.

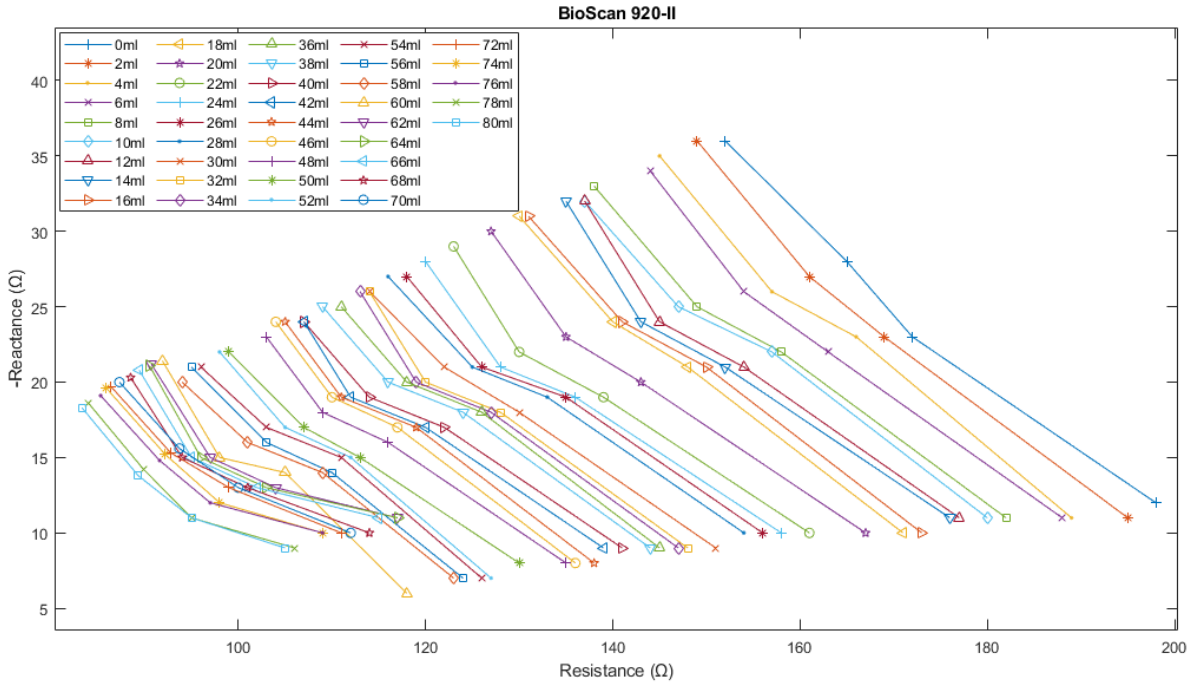

(a)

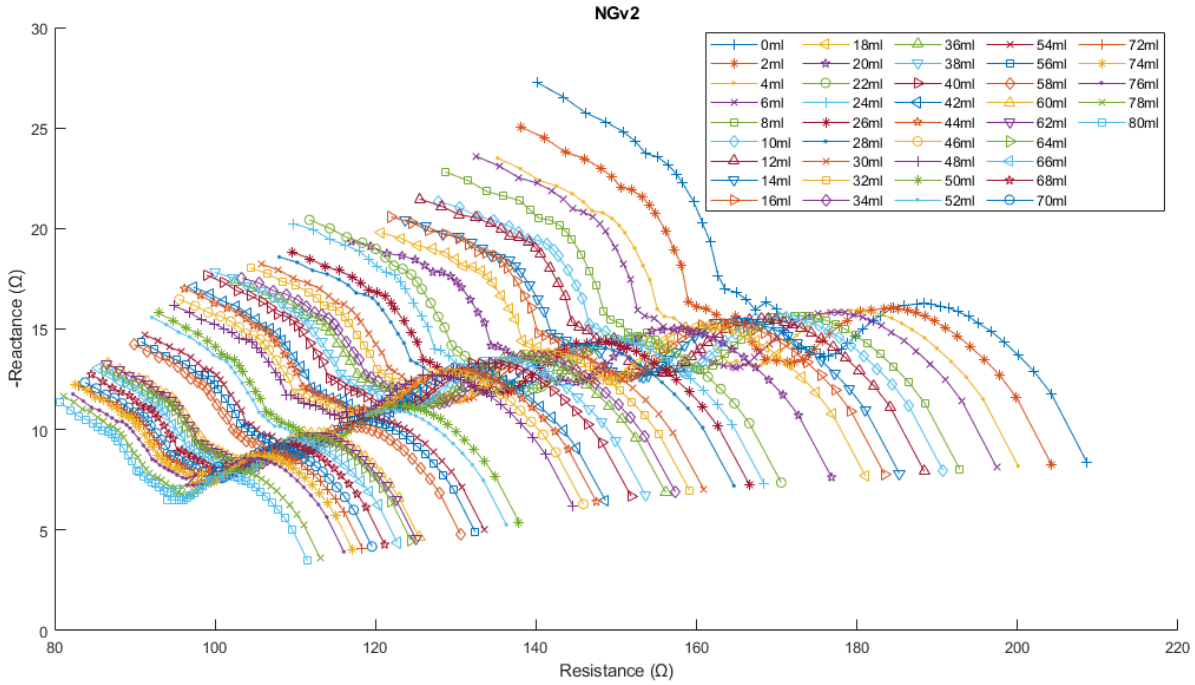

(b)

Figure 4.4: ColeCole plots showing the measured Resistance R and Reactance X of the Meat experiment 2 for each injection step. acquired using: (a) The Maltron BioScan 920-II, (b) The NGv2.

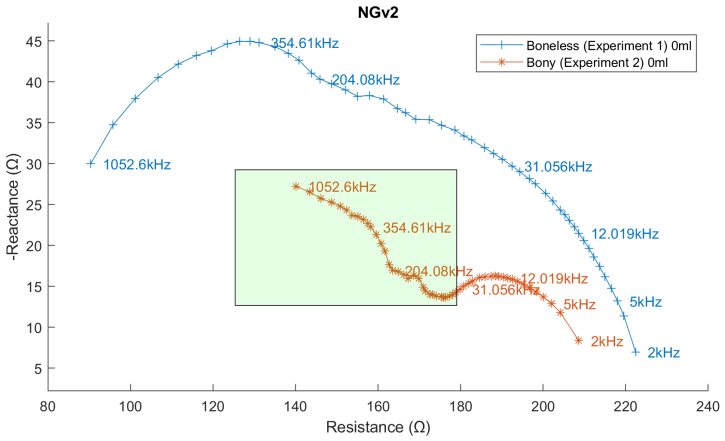

Figure 4.5: Colecole representation highlighting the second bump in reactance in the second meat test (bony) as the frequency increases and comparing it to the first meat experiment (boneless).

4.3 Regressional and Statistical analysis

Goal

The main goal of this analysis to investigate the feasibility of using the dataset acquired from the meat experiments to fit a mathematical model that can be used to predict the amount of added fluid in the biological medium by measuring bio-impedance characteristics. In addition, the secondary goals are to 1. compare the accuracy obtained by a narrow frequency range versus a wider one. 2. to investigate the expediency when relying on the measured bio-impedance of the medium after the presence of a baseline measurement using the fundamentals of impedance ratio (IR) explained in chapter 3.
The second goal will remove the need of measuring bio-impedance on the healthy knee to be used as a baseline for the injured knee.
For this analysis, the datasets acquired from the second meat experiment will be used because it is larger, measured at finer steps, and the biological medium used represents a human knee better.

Datasets

Two main datasets are available:

- The dataset acquired using the Maltron BioScan920-II which contains the measured Resistance $R(\Omega)$ and the Reactance $X(\Omega)$ of the injected current at 4 frequencies ($5kHz, 50kHz, 100kHz$, and $200kHz$) for each step of the 41 injection steps ($0ml - 80ml$, step of $2ml$).
- The dataset acquired using the NGv2 which contains the measured Resistance $R(\Omega)$ and the Reactance $X(\Omega)$ of the injected current at 52 frequencies between $2kHz$ and $1MHz$ for each step of the 41 injection steps ($0ml - 80ml$, step of $2ml$).

Furthermore, the following two properties were added to the datasets as they are being widely used as indications of healthy tissues [Dittmar et al., 2015]:

- The impedance magnitude $|Z|$:

$$\sqrt{ReactanceX^2 + ResistanceR^2}$$

- The phase angle PhA $(degrees)$:

$$tan^{-1}(ReactanceX/ResistanceR)$$

Approach and Pre-Processing

Since the goal is to predict the amount of additional fluid injected into a biological medium, two main approaches will be distinguished:

Using a baseline (Normalized):

This approach will use the measured bio-impedance at $0ml$ hence with no additional fluid injected as a baseline to normalize the rest of the dataset. In which, all other measurements will represent the change in bio-impedance compared to the $0ml$ measurement. In the use case of knee inflammation, the bio-impedance measured on a healthy knee will be used as a baseline for the injured knee.

Without using a baseline (Ratios):

This approach on the other hand eliminates the need to use a baseline and depends on impedance ratio (IR), hence, the ratio of impedance measured at high frequency to impedance measured at low frequency. The study [Rinninella et al., 2018] suggests selecting high and low frequencies according to R_0 and R_∞, respectively. However, in the case of the bony meat test, the impedance curve shows two semi-circles representing two types of cells and therefore it would be hard to determine R_∞.

As an improvement to the impedance ratio (IR) introduced by [Rinninella et al., 2018], a new idea will be tested. Namely, instead of depending on only one impedance ratio, all possible ratios of a high to low frequency will be used. Those ratios can potentially be a good metric since for example, in Figure 4.6, the impedance at frequency $Z(f1)$ represents the impedance of the Extracellular water $Z(ECW)$, while $Z(f2)$ represents the impedance of both the ECW and the impedance of the biological cell type C $Z(ECW) + Z(Cell_{typeC})$, in which, the ratio $Z(f2)/Z(f1)$ can be used to quantify the volume of $Cell_{typeC}$.

Pre-Processing

For each of the approaches described in the previous subsection, a dataset is generated per device, the available datasets become:

- Normalized BioScan920-II: 164 data points (41 measurements, 4 frequencies)
- Normalized NGv2: 2132 data points (41 measurements, 52 frequencies)
- Ratios BioScan920-II: 246 data points (41 measurements, 6 Ratios)
- Ratios NGv2: 54366 data points (41 measurements, 1326 Ratios)

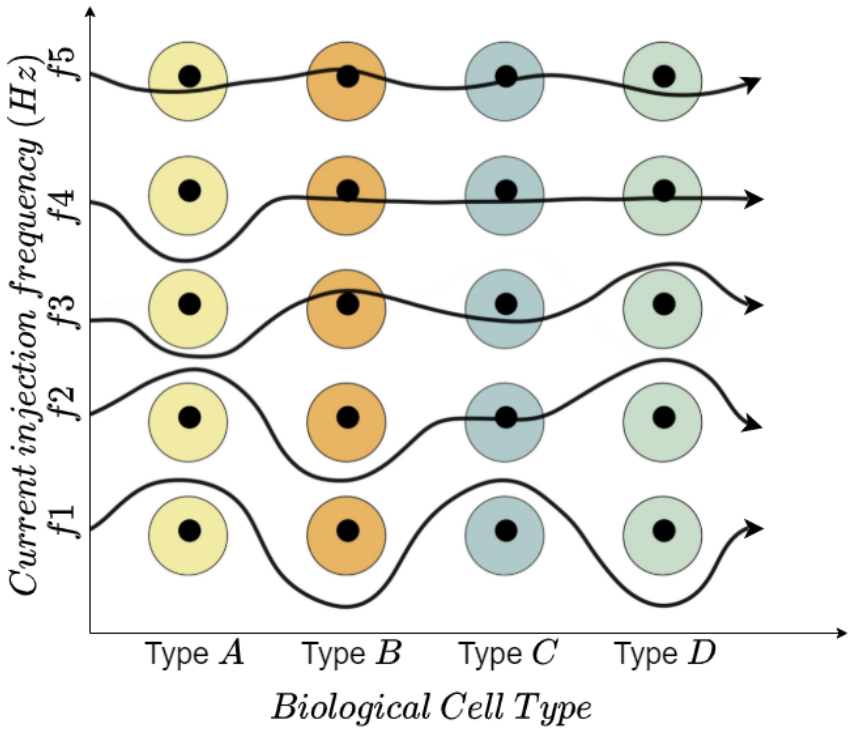

Figure 4.6: An abstract illustration of the relation between frequency increase and the path the injected current will travel through. Such as, when the frequency increases, the current will travel through more types of cells.

Tested models

To explore the feasibility of fitting mathematical models widely, Matlab's Statistics and Machine Learning Toolbox [MATLAB, 2021] is used to explore a variety of regression models. The following functions are used to train the models:

- **fitlm**: *Linear*, *Linear interactions*, and *Linear robust*.
- **fitrnet**: *Narrow NN*, *Medium NN*, and *Wide NN* to train neural networks with a first layer size of *10*, *25*, and *100* respectively.
- **fitrtree**: *Fine Tree*, *Medium Tree*, and *Coarse Tree* to train tree models with a minimum leaf size of *4*, *12*, and *36* respectively.

To train the models, each dataset is split into training and test sets randomly, in which, the test set will contain the data points of one complete measurement step $\cup$ 25% of the dataset, while the training set will contain all remaining data point.

Results

To check for any overfitting, the models are 1. trained 100 times with new randomization of training and test sets. 2. the Root Mean Squared Error (RMSE) of the differences between the predicted volume of fluid and the true volume known of a 5-fold cross-validation [Zhang, 1993] is calculated.
Figures 4.7 and 4.8 present the reported results of the trained models using the normalized and the ratios datasets respectively. It is evident from the results that it

is feasible to use fitted mathematical models to predict the volume of added fluids in a human knee biological medium. The most accurate fitting was reached when the normalize dataset from the device with the wide frequency range was used.

Frequency range

The results obtained when using the normalized datasets shows that having a wider frequency range will directly contribute to the accuracy of the fitting as the overall R^2 of the training set is 0.92 ± 0.0455 and 0.85 ± 0.144 for the NGv2 and Maltron BioScan920-II respectively. Moreover, the RMSE of the 5-fold cross-validation also confirms the latter result as the overall RMSE is $1.82 \pm 1.07(ml)$ and $3.5 \pm 3.42(ml)$ for the normalized tests of the NGv2 and Maltron BioScan920-II respectively.

With or without using a baseline

Furthermore, the results obtained using the proposed ratios dataset shows low R^2 and large fluctuations with an overall of 0.51 ± 0.348 and 0.42 ± 0.140 for the NGv2 and Maltron BioScan920-II respectively, along with the high RMSE of $11.5 \pm 8.2(ml)$ and $13.6 \pm 3.3(ml)$ for the same devices, indicates that the tested *Ratios* approach could not fit a suitable model from the tested regression models

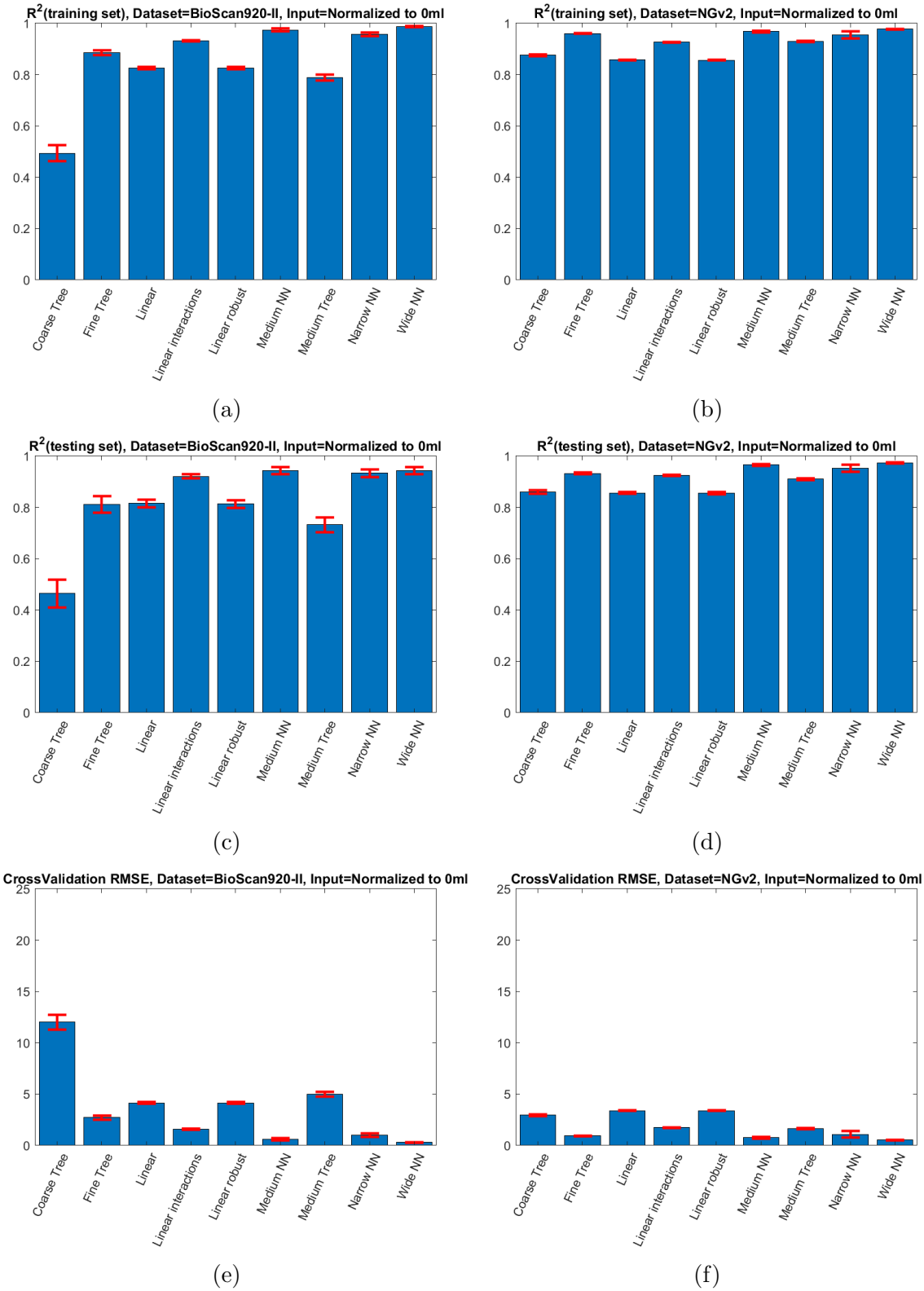

Figure 4.7: Average (in blue) and standard deviation (in red) of the R^2 and the absolute cross-validation RMSE (ml) of the training and the test set of the datasets Normalized BioScan920-II and Normalized NGv2, trained 100x with random splits of test and training input data sets

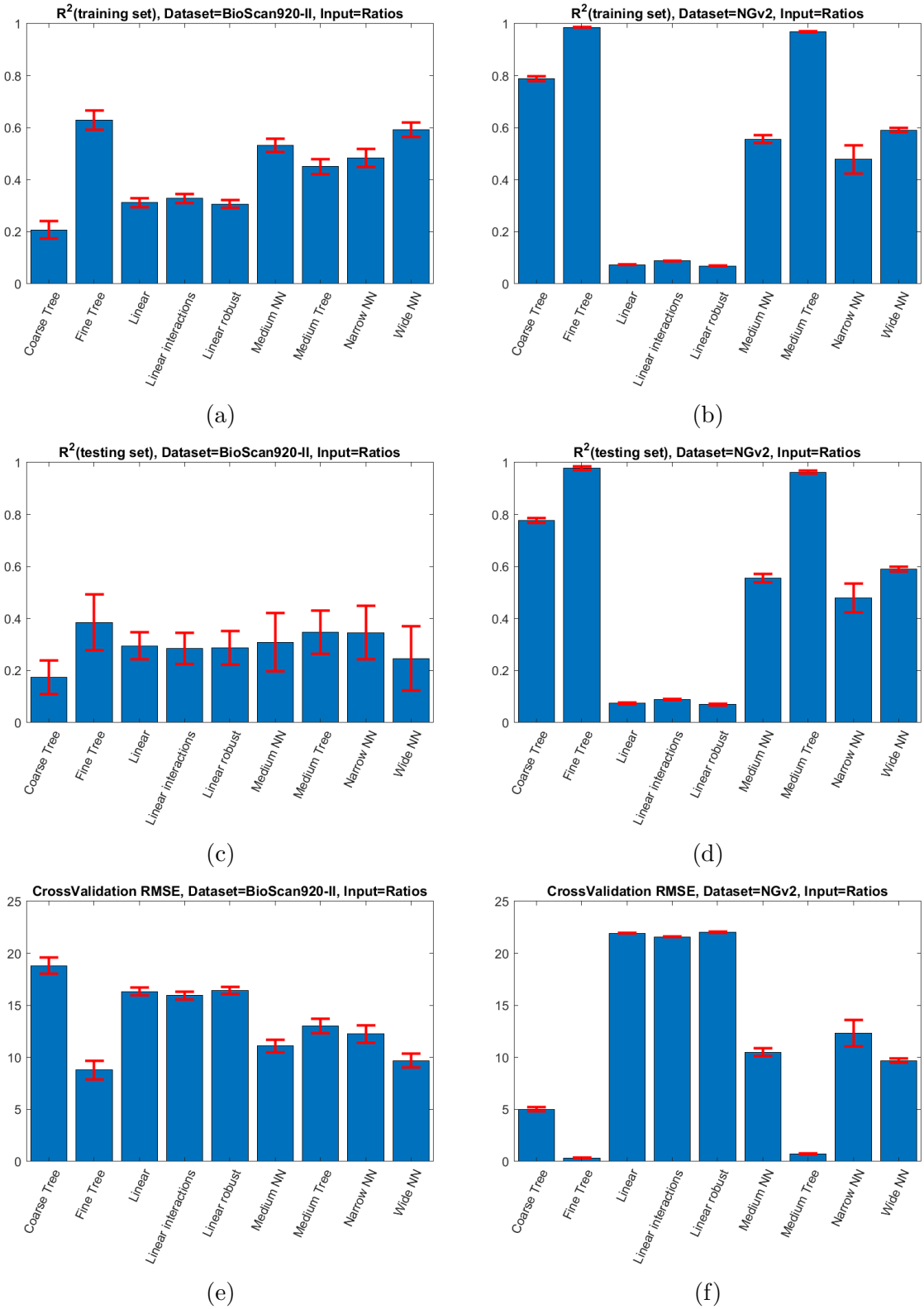

Figure 4.8: Average (in blue) and standard deviation (in red) of the R^2 and the absolute cross-validation RMSE (ml) of the training and the test set of the datasets Ratios BioScan920-II and Ratios NGv2, trained 100x with random splits of test and training input data sets

Chapter 5

Knee Brace proposal

5.1 Material and design

In order to achieve the goal of developing a wearable measurement device, it is important to take into consideration the ease of use of the setup by patients and physiotherapists to achieve a minimum probability of measurement errors and maximal clinical acceptability. As described in section (3.4) the gel electrodes are, in perfect conditions, considered the gold standard. However, those conditions are usually in the context of clinics and hospitals where experts can make sure to shave and clean the body part interested to the measurement. Furthermore, in the hospital, the electrodes are correctly placed by the experts to avoid even little misplacement errors that could affect the result. As the setup is ultimately meant to be used by physiotherapists or by patients themselves at home to monitor the changes during the recovery period, the multiple measurements related to the same patient need to be acquired with the same set-up. This condition cannot be provided if the position of the electrodes changes at each acquisition. Therefore, in this work, a custom knee brace with a fixed type and placement of the electrodes is proposed to standardize the measurements.

As a starting point, we used one of the commercially available known knee braces that are used by athletes and patients with knee pathology as those braces proven to reduce pain during the recovery period of the joint [Brandsson et al., 2001].

Using silver woven conductive fabric made of silver-plated nylon with a resistance of less than 1Ω per 30 cm, we made four strips of 1x30 sewed to the inner side of the brace. Push-button connectors are added to create an interface where leads can be connected from the outside. In the first iterations, we started with straight line stitches. However as the conductive fabric is very sensitive to tearing especially around its edges, some threads were torn, That can potentially affect the measurement significantly especially if threads from one electrode touch another, see Figure 5.2. To solve this problem, the edges of the fabric were bend and sewn using zigzag stitches. In this way, the brace has been functioning great even after more than 50 tests.

(a)

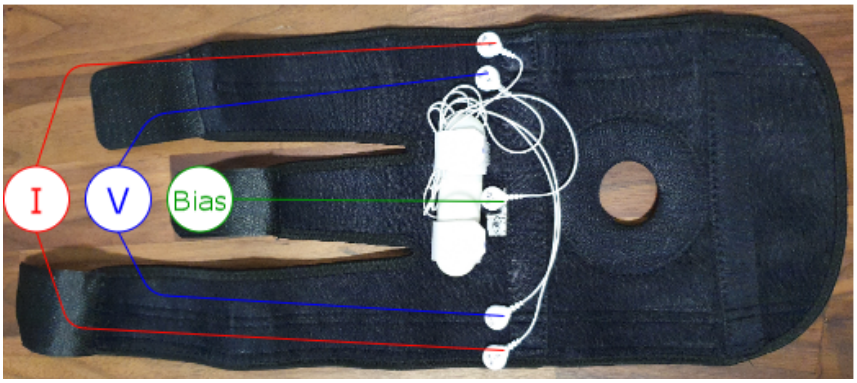

(b)

Figure 5.1: The custom brace, (a) the inner-side with the conductive fabric stitched. (b) the outer-side showing the button connectors used to connect bio-impedance measuring instruments

5.2 Evaluation on Patients

5.2.1 Study Description

The goal of this evaluation is to investigate the performance of the custom knee brace by comparing the measured impedance to traditional electrodes and to determine the validity of using multi-frequency bio-impedance to measure the volume of swelling by comparing the resistance measured on the injured knee to the healthy contralateral knee. Ten patients of TopSupport, the physiotherapy department of St.Anna Hospital in Eindhoven volunteered to participate in the study. 8 Males and 2 Females (Age=$30 \pm 12 years$, Height=$182 \pm 8 cm$, Mass=$84 \pm 23 kg$). All participating subjects were recovering from knee trauma and/or knee surgery with an inflamed knee as a result, 9 had gone through medical intervention (70 ± 63 days since medical intervention), 7 had an Anterior Cruciate Ligament (ACL) injury, 1 had Quad tendon rupture, and 2 had both ACL and a Torn Meniscus. Only one patient did not have a medical intervention yet. More information about the patients involved in the study can be found in the Appendix (7.2). The Maltron BioScan920-II [Maltron International, 2021] is used to measure bio-impedance at four frequencies (5kHz, 50kHz, 100kHz, and 200kHz) and a compact SEEK thermal camera [Seek Thermal, 2021] is used to measure skin temperature for reference. The experiment was reviewed and evaluated by the internal ethical committee of IMEC

Figure 5.2: A photograph showing the torn threads of the conductive fabric

and the Medical ethical committee of the Maxima Medisch Centrum (MMC).

5.2.2 Experiment Protocol

Patients are first informed about the goals of the study, the measurement procedure, and the expected total duration. After signing an informed consent form, due to the current Covid-19 pandemic, the patient is instructed to perform some of the steps him/herself.

The following steps are done by the patient unless otherwise is explicitly mentioned.

- Measure the circumference at 1 cm above the cap of the patella.
- Put on the knee brace on one of the knees.
- Relax and lay supine for 5 minutes to ensure that body fluid is stabilized,
- The investigator will do a bio-impedance measurement.
- Move the knee brace to the other knee and relax in supine for 5 minutes.
- The investigator will do a bio-impedance measurement.
- Remove the knee brace and clean the skin with 70% isopropyl alcohol preparation pads.
- Place commercially available standard Ag/Agcl electrodes on both knees using a brace template to position electrodes at the same spacing as the brace.
- The investigator will do a bio-impedance measurement and repeat it for both knees.
- Remove the electrodes.
- The investigator will lastly measure the skin temperature of both knees using a thermal camera.

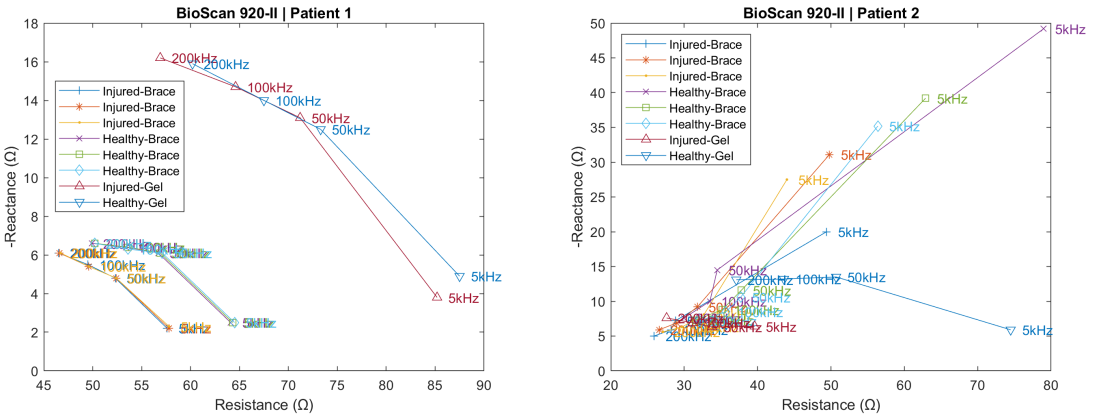

(a) (b)

Figure 5.3: The measured impedance on both injured and healthy contralateral knees of patients with ACL injuries using traditional gel electrodes and the custom brace, the measurement with the brace is repeated 3 times per patients per knee to check the consistence of the results. Patient P1 (a) had much less hairy skin compared to Patient P2 (b)

5.2.3 Results and Discussion

Patients were not asked to explicitly shave the knee area to participate in this study. While most of them had a normal hair level, Patient 2 had very hairy skin which affected the measured impedance significantly and therefore will be excluded from the results see Figure 5.3 b. Furthermore, due to the larger electrode-to-skin surface area of the brace, the overall measured impedance was lower than the traditional gel electrodes with ($22 \pm 6.5\Omega$, $15 \pm 7.8\Omega$, $12.8 \pm 8.3\Omega$, $11 \pm 8.4\Omega$) lower average resistance for the frequencies ($5kHz$, $50kHz$, $100kHz$, and $200kHz$). Also, as expected, the injured and swollen knees of all patients had lower resistance and reactance compared to the healthy contralateral knee when tested with both the traditional electrodes and the knee brace. In addition, the larger surface area of the electrodes in the brace is expected to have helped in reducing the measurement noise as well which led to a more clear difference between the impedance of injured knee and the healthy contralateral knee compared to the gel electrodes see Figure 5.3 a. For complete results see Appendix 7.3. To check the repeatability of the measurements using the brace, the same test was repeated 3 times on each knee, the overall average standard deviation of the 3 measurements on each knee was 0.268Ω and 0.127Ω for the Resistance and Reactance respectively. While the deviation was very low, it is noticeable that the was proportional to the frequency of injected current shown in Figure 5.4

While the models in chapter 4 are based on the datasets acquired from a test on an ex vivo porcine model, the fitted coefficients of one of the best performing models, the *Linear interaction* are used to try to predict the volume of swelling in the injured knee of the patients. Using the healthy knee as a baseline, table 5.1 shows the average predicted volume of additional fluids in ml in the injured knee compared to the healthy contralateral knee. The results show a good correlation between the expert's assessment and the average predicted swelling volume as for

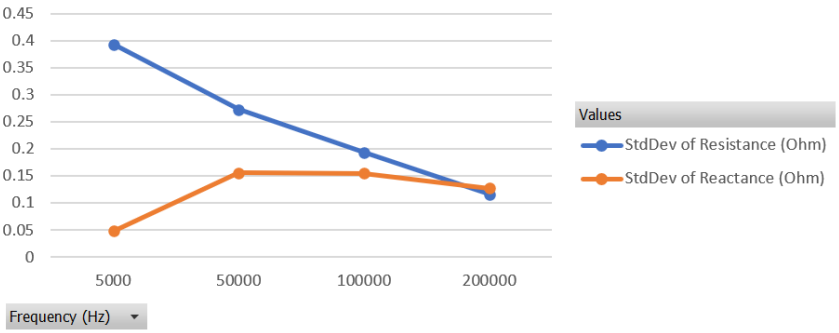

Figure 5.4: The average standard deviation in measured Resistance and Reactance per frequency for each 3 measurements using the brace on the same knee for the patients (excluding patient 2)

example, the highest volume of predicted swelling of 17.3ml was for the patient P5 and the swelling was scored the worst by the expert as well.

The outliers we see are P8 and P9. However, when we compare the number of days since the medical intervention to other patients, we notice that patient P8 did not have surgery yet and patient P9 was operated more than 8 months ago. An orthopedic expert suggests that the swelling in patient P9 is a result of inflammatory scar tissue and more superficial [Chan et al., 2015]

Table 5.1: Average and standard deviation of predicted volume (ml) of additional fluids in the injured knee using the healthy knee as a baseline evaluated using the Linear Interaction model trained 100 times with random splits of test and training input data sets

Patient (note)	***Average Predicted (ml)***	***StdDev of Predicted (ml)***	***Days since medical intervention***	***Circumference (cm) (injured - contralateral)***	***Skin temperature (°) (injured - contralateral)***	***Expert's assessment (0-3)***	***Patient's swelling assessment (0-10)***
P1	5.507	2.53	60	0.40	2.00		3
P2 (very hairy)	-61.475	101.44	46	1.00	3.00		5
P3	7.889	1.88	51	0.60	4.00		
P4	11.183	1.79	66	0.50	2.00	1	5
P5	17.321	2.25	105	1.10	3.00	3	5
P6	14.069	5.87	68	3.00	4.00	2	7
P7	11.786	1.94	52	2.90	0.00	1	7
P8	-0.315	1.89	N/A	0.30	1.00	2	
P9	-0.054	1.67	234	0.70	4.00	1	3
P10	13.497	2.40	25	0.60	3.00	2	4

Chapter 6

Conclusion and Future work

This work aimed to study and prove the feasibility of developing a wearable to evaluate the health of a knee joint after an inflammatory response using bio-impedance. Based on the results provided, it is proven that it is feasible to develop a wearable that can be used to evaluate the health of a knee joint after an inflammatory response using bio-impedance. Furthermore, based on ex vivo experiments, we show that fitting a mathematical model to predict the volume of fluid accumulated in the knee is achievable as it was able to distinguish a variation as low as $2ml$. The latter is expected to provide a more objective assessment compared to the current assessments that are highly dependent on physiotherapists. Moreover, for a truly wearable system, we show that is it possible to use conductive fabric attached to a knee brace to eliminate the burden of using the traditional pre-gelled single-use electrodes.

Limitations

- The dataset used for regression analysis is acquired from a porcine model. A larger dataset and preferable acquired from human models is expected to result is more accurate models for the target application.
- We showed in chapter 4 that more frequencies can improve the accuracy of predictions. However, within the available time, it was not possible to approve the use of the NGv2 with the custom brace for bio-impedance measurements on human subjects. as a result, we were limited to using the Maltron BioScan920-II for measurements on patients.
- Due to the current pandemic (Covid-19) the number of participating patients was limited to 10.

Future work

A suggested path for related future work would be including more types of sensors in the brace to measure temperature, redness, and circumference to improve the accuracy of predictions. In addition, we noticed during the project that medical experts find it difficult to relate the volume of fluid in ml to swelling level as it is highly dependent on the BMI of the patient, therefore, introducing a new metric that can combine and relate the fluid level to BMI is interesting to explore.

Bibliography

[Aasvang et al., 2015] Aasvang, E. K., Luna, I. E., and Kehlet, H. (2015). Challenges in postdischarge function and recovery: the case of fast-track hip and knee arthroplasty. *BJA: British Journal of Anaesthesia*, 115(6):861–866.

[Azar, 2012] Azar, A. T. (2012). *Modeling and Control of Dialysis Systems: Solutions Manual* .

[Brandsson et al., 2001] Brandsson, S., Faxen, E., Kartus, J., Eriksson, B., and Karlsson, J. (2001). Is a knee brace advantageous after anterior cruciate ligament surgery? a prospective, randomised study with a two-year follow-up. *Scandinavian journal of medicine & science in sports*, 11(2):110–114.

[Casteleyn, 1999] Casteleyn, P.-P. (1999). Acute knee injuries: diagnostic & treatment management proposals.

[Chan et al., 2015] Chan, D. D., Xiao, W., Li, J., de la Motte, C. A., Sandy, J. D., and Plaas, A. (2015). Deficiency of hyaluronan synthase 1 (has1) results in chronic joint inflammation and widespread intra-articular fibrosis in a murine model of knee joint cartilage damage. *Osteoarthritis and cartilage*, 23(11):1879–1889.

[Dellis, 2021] Dellis, J.-L. (2021). *version 1.3*. MATLAB Central File Exchange.

[Denoble et al., 2010] Denoble, A. E., Hall, N., Pieper, C. F., and Kraus, V. B. (2010). Patellar skin surface temperature by thermography reflects knee osteoarthritis severity. *Clinical Medicine Insights: Arthritis and Musculoskeletal Disorders*, 3:CMAMD–S5916.

[Dittmar et al., 2015] Dittmar, M., Reber, H., and Kahaly, G. (2015). Bioimpedance phase angle indicates catabolism in type 2 diabetes. *Diabetic Medicine*, 32(9):1177–1185.

[Gabriel et al., 1996] Gabriel, S., Lau, R., and Gabriel, C. (1996). The dielectric properties of biological tissue ii: Measurements in the frequency range 10 hz to 20 ghz. *Physics in medicine and biology*, 41:2251–69.

[Golowasch and Nadim, 2013] Golowasch, J. and Nadim, F. (2013). *Capacitance, Membrane*, pages 1–5. Springer New York, New York, NY.

[Grimnes and Martinsen, 2010] Grimnes, S. and Martinsen, Ø. G. (2010). Alpha-dispersion in human tissue. *Journal of Physics: Conference Series*, 224:012073.

[Harres, 2013] Harres, D. (2013). Chapter 3 - beginning electronics – resistors, capacitors, and inductors. In Harres, D., editor, *MSP430-based Robot Applications*, pages 17–42. Newnes, Oxford.

[Hootman et al., 2002] Hootman, J. M., Macera, C. A., Ainsworth, B. E., Addy, C. L., Martin, M., and Blair, S. N. (2002). Epidemiology of musculoskeletal injuries among sedentary and physically active adults. *Medicine and science in sports and exercise*, 34(5):838–844.

[Instruments, 2007] Instruments, G. (2007). Basics of electrochemical impedance spectroscopy. *G. Instruments, Complex impedance in Corrosion*, pages 1–30.

[Jakobsen et al., 2010] Jakobsen, T. L., Christensen, M., Christensen, S. S., Olsen, M., and Bandholm, T. (2010). Reliability of knee joint range of motion and circumference measurements after total knee arthroplasty: does tester experience matter? *Physiotherapy Research International*, 15(3):126–134.

[Jaremko et al., 2017] Jaremko, J. L., Jeffery, D., Buller, M., Wichuk, S., McDougall, D., Lambert, R. G., and Maksymowych, W. P. (2017). Preliminary validation of the knee inflammation mri scoring system (kimriss) for grading bone marrow lesions in osteoarthritis of the knee: data from the osteoarthritis initiative. *RMD Open*, 3(1).

[Lee et al., 2019] Lee, S., Grundlehner, B., van der Westen, R. G., Polito, S., and Van Hoof, C. (2019). Nightingale v2: Low-power compact-sized multi-sensor platform for wearable health monitoring. In *2019 41st Annual International Conference of the IEEE Engineering in Medicine and Biology Society (EMBC)*, pages 1290–1293.

[Lieberman et al., 2021] Lieberman, E. G., Barrack, R. L., and Schmalzried, T. P. (2021). Suspected metal allergy and femoral loosening after total knee arthroplasty: A diagnostic dilemma. *Arthroplasty Today*, 7:114 – 119.

[Loyd et al., 2020] Loyd, B. J., Kittelson, A. J., Forster, J., Stackhouse, S., and Stevens-Lapsley, J. (2020). Development of a reference chart to monitor postoperative swelling following total knee arthroplasty. *Disability and Rehabilitation*, 42(12):1767–1774. PMID: 30668214.

[Maltron International, 2021] Maltron International (2021). Bioscan 920 - ii — body composition machine.

[Maricar et al., 2016] Maricar, N., Callaghan, M. J., Parkes, M. J., Felson, D. T., and O'Neill, T. W. (2016). Clinical assessment of effusion in knee osteoarthritis—a systematic review. *Seminars in Arthritis and Rheumatism*, 45(5):556 – 563.

[MATLAB, 2021] MATLAB (2021). *version 9.9.0 (R2020b)*. The MathWorks Inc., Natick, Massachusetts.

[McDonald et al., 2012] McDonald, D., Siegmeth, R., Deakin, A., Kinninmonth, A., and Scott, N. (2012). An enhanced recovery programme for primary total knee arthroplasty in the united kingdom—follow up at one year. *The Knee*, 19(5):525–529.

[Mellert et al., 2011] Mellert, F., Winkler, K., Schneider, C., Dudykevych, T., Welz, A., Osypka, M., Gersing, E., and Preusse, C. J. (2011). Detection of (reversible) myocardial ischemic injury by means of electrical bioimpedance. *IEEE Transactions on Biomedical Engineering*, 58(6):1511–1518.

[Muller et al., 2020] Muller, T., Ward, L., Plush, K., Pluske, J., D'Souza, D., Bryden, W., and van Barneveld, R. (2020). Use of bioelectrical impedance spectroscopy to provide a measure of body composition in sows. *Animal*, page 100156.

[Rinninella et al., 2018] Rinninella, E., Cintoni, M., Addolorato, G., Triarico, S., Ruggiero, A., Perna, A., Silvestri, G., Gasbarrini, A., and Mele, M. (2018). Phase angle and impedance ratio: Two specular ways to analyze body composition. *Annals of Clinical Nutrition*, 1.

[Roa et al., 2013] Roa, L. M., Naranjo, D., Reina-Tosina, J., Lara, A., Milán, J. A., Estudillo, M. A., and Oliva, J. S. (2013). *Applications of Bioimpedance to End Stage Renal Disease (ESRD)*, pages 689–769. Springer Berlin Heidelberg, Berlin, Heidelberg.

[Roemer et al., 2016] Roemer, F., Jarraya, M., Felson, D., Hayashi, D., Crema, M., Loeuille, D., and Guermazi, A. (2016). Magnetic resonance imaging of hoffa's fat pad and relevance for osteoarthritis research: a narrative review. *Osteoarthritis and Cartilage*, 24(3):383 – 397.

[Seek Thermal, 2021] Seek Thermal (2021). Seek thermal — thermal imaging cameras.

[Steinbrueck, 1999] Steinbrueck, K. (1999). Epidemiology of sports injuries - 25-year-analysis of sports orthopedic-traumatologic ambulatory care. *sports injury sports damage: organ of the Society for Orthopadic-Traumatological Sports Medicine*, 13(2):38–52.

[Wang et al., 2019] Wang, Y., Martel-Pelletier, J., Teichtahl, A. J., Wluka, A. E., Hussain, S. M., Pelletier, J.-P., and Cicuttini, F. M. (2019). The bulge sign – a simple physical examination for identifying progressive knee osteoarthritis: data from the Osteoarthritis Initiative. *Rheumatology*, 59(6):1288–1295.

[Weik, 2001] Weik, M. H. (2001). *impedance, resistance, and capacitive reactance.* Springer US, Boston, MA.

[Zhang, 1993] Zhang, P. (1993). Model selection via multifold cross validation. *The annals of statistics*, pages 299–313.

[Zschäbitz et al., 1992] Zschäbitz, A., Neurath, M., Grevenstein, J., Koepp, H., and Stofft, E. (1992). Correlative histologic and arthroscopic evaluation in rheumatoid knee joints. *Surgical endoscopy*, 6(6):277–282.

List of Figures

Chapter 7

Appendix

7.1 Comparing the accuracy of the NGV2 and the Oxpecker V1.1

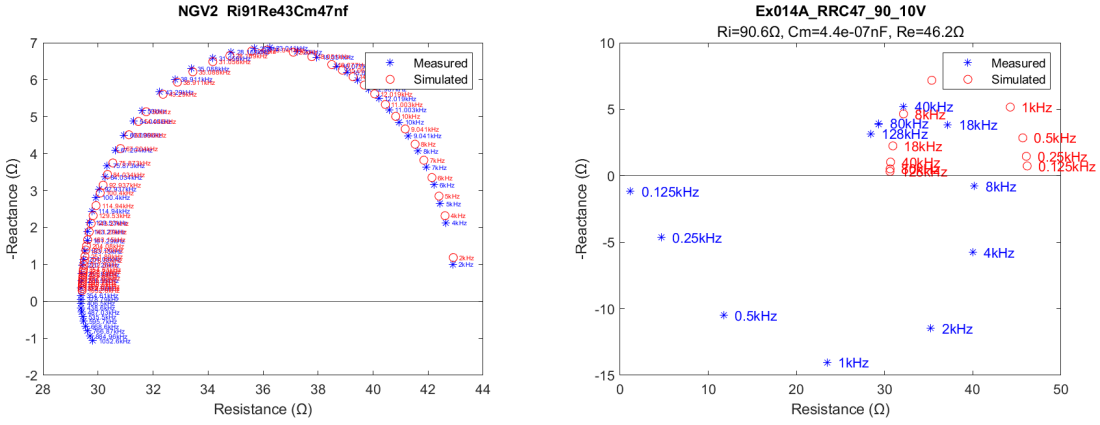

(a)

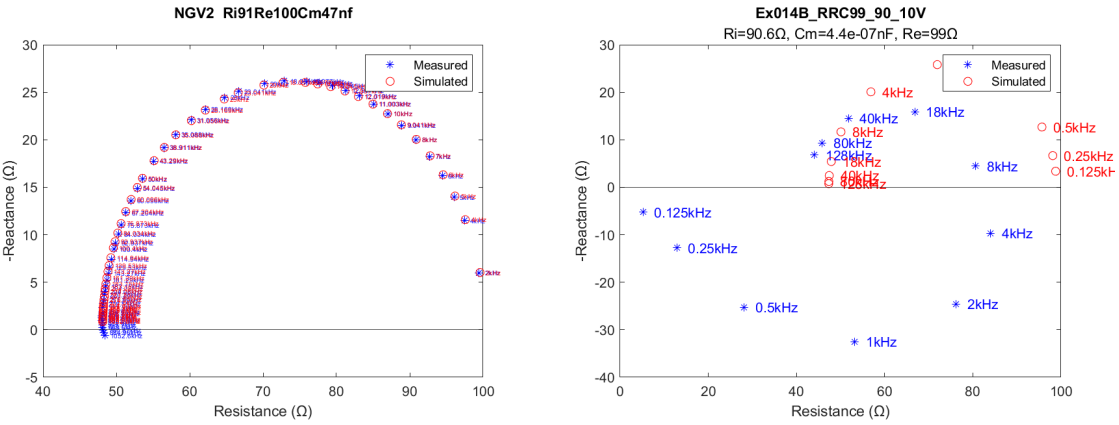

(b)

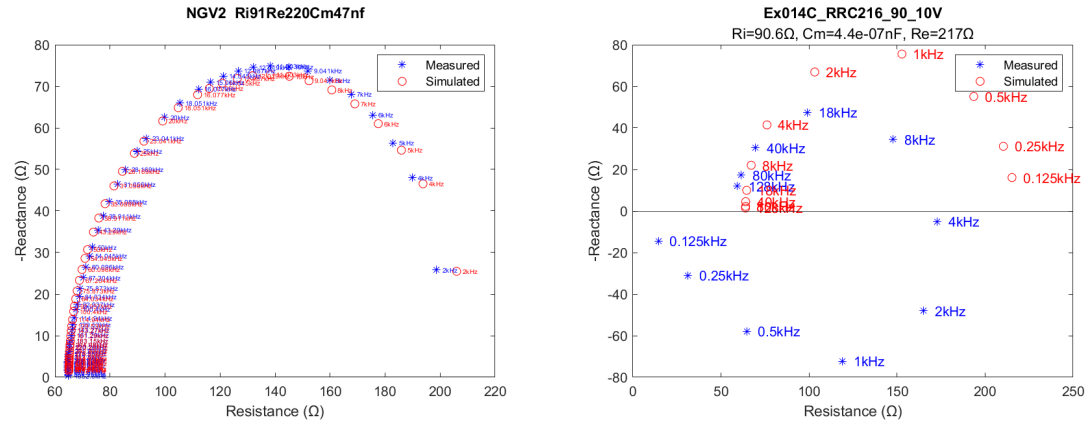

(c)

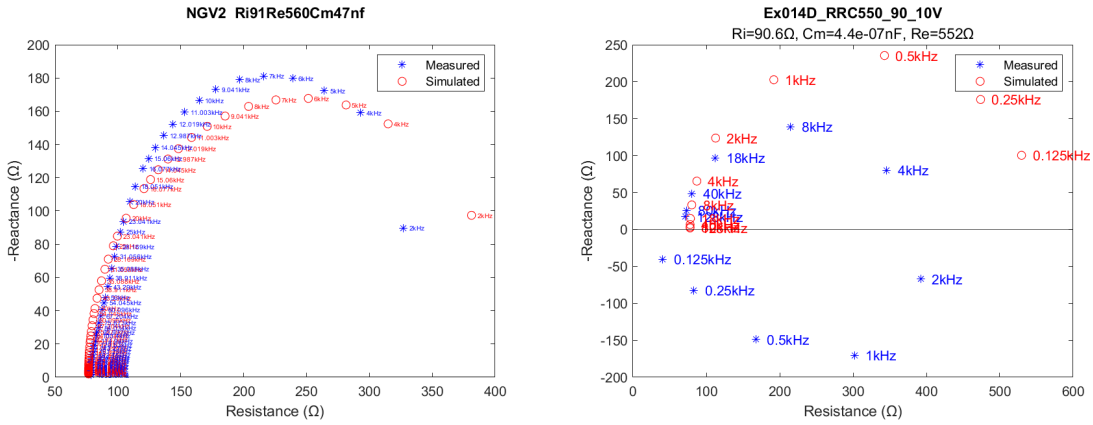

(d)

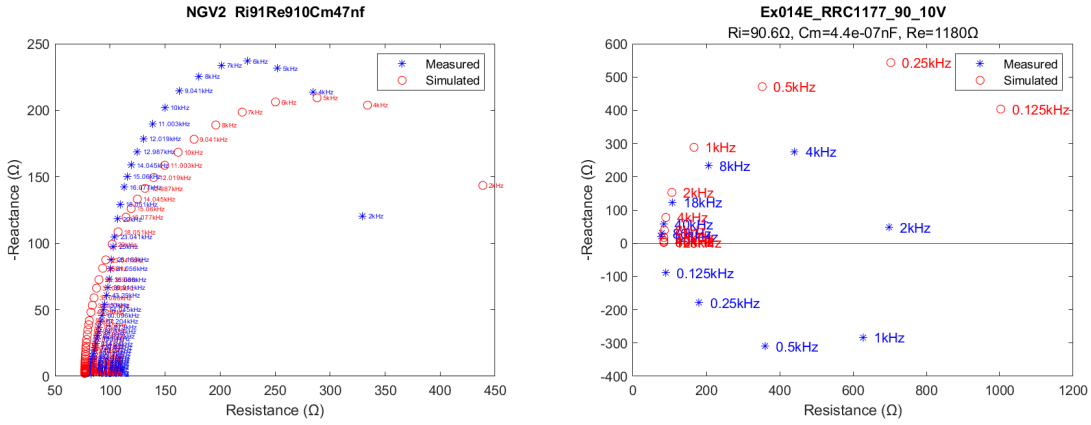

(e)

Figure 7.1: Comparing the accuracy of on the left side, the Nightingale V2 (NGV2) at 52 frequencies in the range of [2 kHz - 1 MHz] and on the right side, the Oxpecker at 11 frequencies in the range of [125 Hz - 128 kHz] when measuring the impedance of an equivalent circuit from figure 3.3 with multiple R_e resistors compared to the expected impedance from the simulation fitted by Zfit [Dellis, 2021]. The exact measured components are given above each sub-figure.

7.2 Patients' characteristics

Table 7.1: Patients' characteristics

Patient	***Injured Knee (R/L)***	***Injury type***	***Days since medical intervention***	***BMI*** (kg/m^2)	***Age group (years)***	***Gender (M/F)***	***Skin temperature***	***Circumference (cm)***	***Patient swelling assessment (0-10)***	***Expert assessment (0-3)***
P1	R	ACL	60	20.2	(20-30)	Female	R=29° L=27°	R=38.4 L=38	3	
P2	L	ACL	46	24.8	(30-40)	Male	R=28° L=31°	R=38.4 L=39.4	5	
P3	R	ACL Torn meniscus	51	22.2	(20-30)	Male	R=30° L=26°	R=39.8 L=39.2		
P4	L	ACL	66	23	(30-40)	Male	R=28° L=30°	R=38.2 L=39.7	5	1
P5	R	Quad tendon rupture	105	31.2	(60-70)	Male	R=31° L=28°	R=47.9 L=46.8	5	3
P6	R	ACL	68	38,3	(20-30)	Male	R=32° L=28°	R=54.7 L=51.7	7	2
P7	R	ACL	52	26,8	(20-30)	Male	R=30° L=30°	R=44.3 L=41.4	7	1
P8	R	ACL	N/A	18.9	(10-20)	Female	R=31° L=30°	R=37.5 L=37.2		2
P9	R	ACL	234	23.9	(20-30)	Male	R=31° L=27°	R=38.5 L=37.8	3	1
P10	R	ACL Torn Meniscus	25	21.2	(10-20)	Male	R=31° L=28°	R=39.3 L=38.7	4	2

7.3 Patients' measured impedance

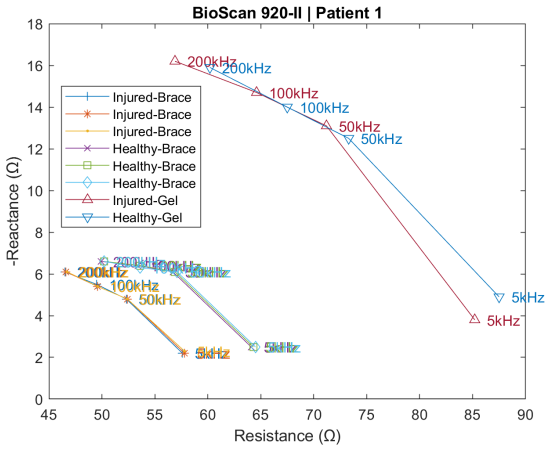

(a)

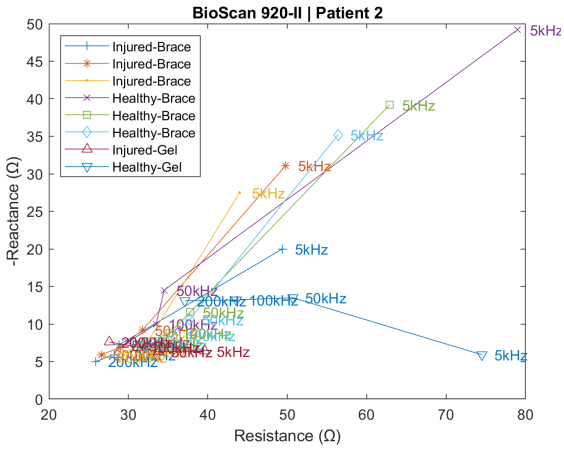

(b)

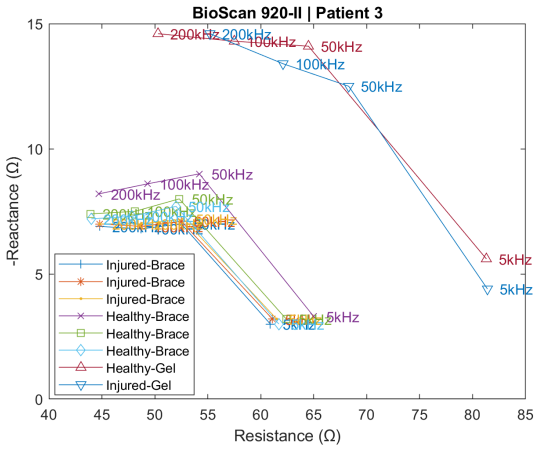

(c)

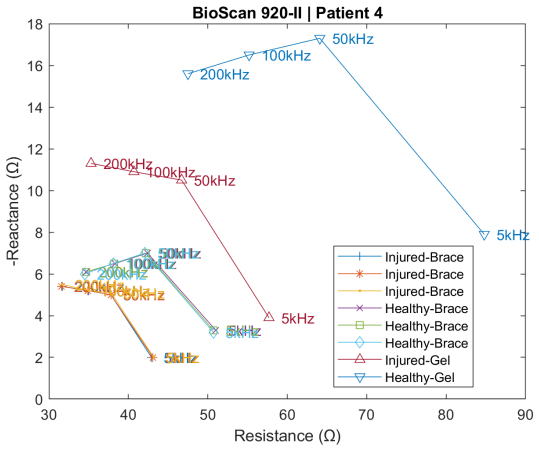

(d)

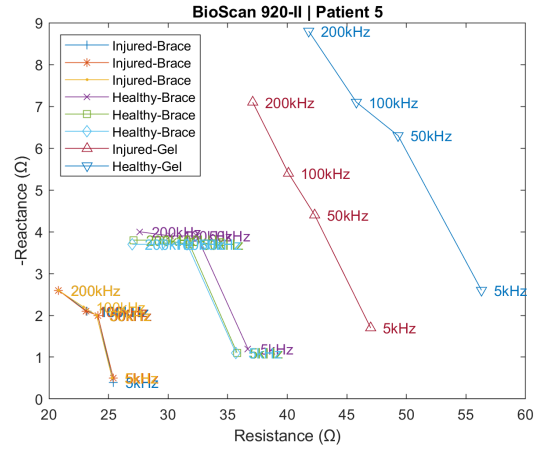

(e)

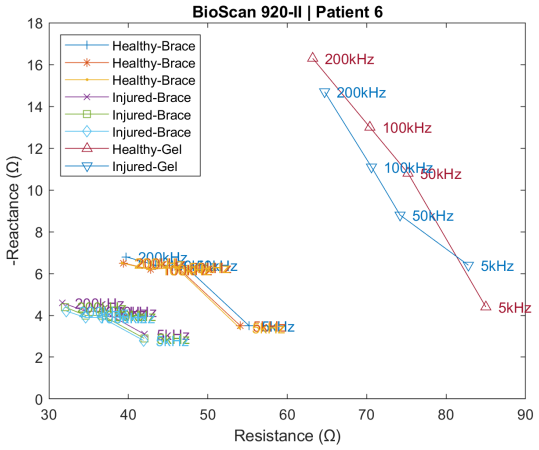

(f)

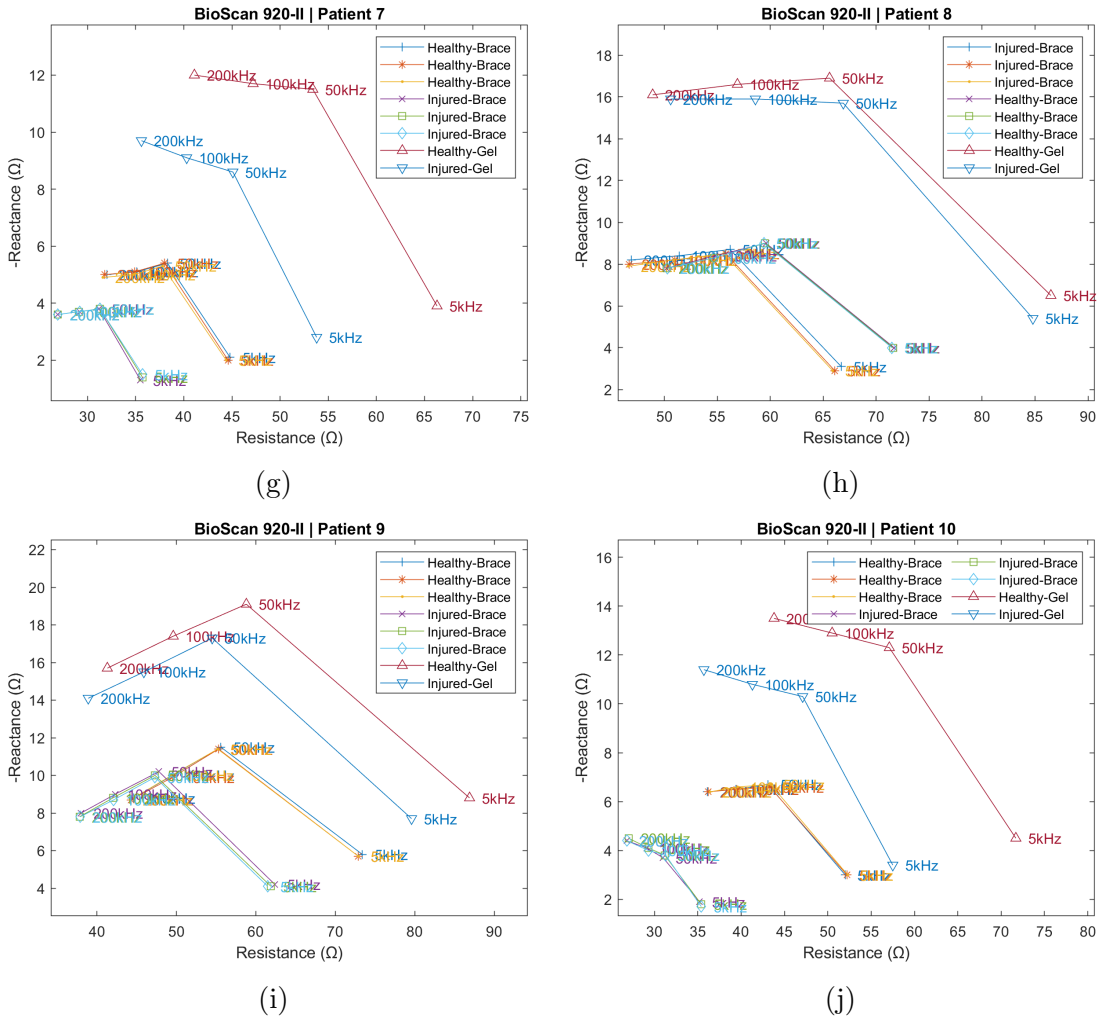

Figure 7.2: Colecole representation of the bio-impedance measure on both knees of patients with known knee injures. **Note:** the results in (b) are included to show how a very hairy skin can affect the accuracy of the acquired data significantly.